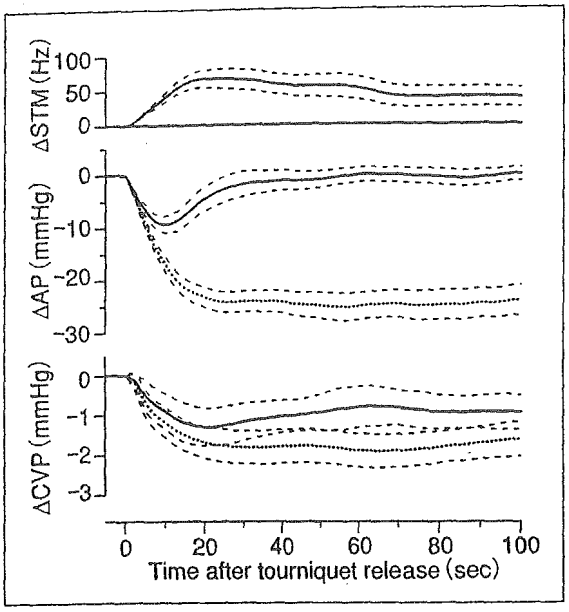

図5　圧迫止血帯の急激な解除に伴う急激な血圧低下
バイオニック動脈圧反射装置が作動していない場合(点線)には，圧迫止血帯の解除に伴い急激に血圧(AP)と中心静脈圧(CVP)が低下したが，バイオニック動脈圧反射が作動している場合(実線)には，両者ともに低下が抑制された．破線は平均±標準偏差(22例)を示す．

唆している．したがって，このような，10秒以内に血圧が20mmHg低下するモデルは，バイオニック動脈圧反射装置の有効性を評価するために妥当であると考えられた．

図から明らかなように，バイオニック動脈圧反射装置が作動している場合には，圧迫止血帯の解除に伴う急激な血圧低下は，数秒以内に食い止められ，止血帯解除前の血圧値にすみやかに回復した．以上のような結果から，バイオニック動脈圧反射装置は，本モデルのような血圧低下に対しては有用であると考えられた．

ま と め

起立性低血圧などのような血圧調節障害に対する治療法として，輸液・輸血法，薬物療法，機械的サポート法などが知られているが，本稿で紹介した手法はこれらとは異なり，自律神経系とインターフェイスして，医工学的に動脈圧反射機能を再建しようとするものである．その利点は，神経性であるがゆえに迅速な調節が可能であるだけでなく，オンデマンド的動作であるため，不要な臥位高血圧をまねく危険性が少ないことも期待される．

バイオニック動脈圧反射装置を臨床応用するにあたっては，長期使用の可能な交感神経刺激電極の開発や小型電気刺激装置が必要となるが，すでに難治性てんかんの治療用としてカフ型の迷走神経刺激電極や刺激装置が開発され，多くの症例に使用されている[18]．したがって，このような要素技術を応用すれば，バイオニック動脈圧反射装置が起立性低血圧の治療器として実用化できるかもしれない．

文　献

1) Robertson D. Diagnosis and management of baroreflex failure. Primary Cardiol 1995 ; 21 : 37.
2) The Consensus Committee of the American Autonomic Society and the American Academy of Neurology. Consensus statement on the definition of orthostatic hypotension, pure autonomic failure, and multiple system atrophy. Neurology 1996 ; 46 : 1470.
3) Ketch T, Biaggioni I, Robertson R, et al. Four faces of baroreflex failure : hypertensive crisis, volatile hypertension, orthostatic tachycardia, and malignant vagotonia. Circulation 2002 ; 105 : 2518.
4) Bannister R, da Costa DF, Hendry WG, et al. Atrial demand pacing to protect against vagal overactivity in sympathetic autonomic neuropathy. Brain 1986 ; 109 : 345.
5) Kristinsson A. Programmed atrial pacing for orthostatic hypotension. Acta Med Scand 1983 ; 214 : 79.
6) Sato T, Kawada T, Shishido T, et al. Novel therapeutic strategy against central baroreflex failure : a bionic baroreflex system. Circulation 1999 ; 100 : 299.
7) Sato T, Kawada T, Sugimachi M, et al. Bionic technology revitalizes native baroreflex function in rats with baroreflex failure. Circulation 2002 ; 106 : 730.
8) Yanagiya Y, Sato T, Kawada T, et al. Bionic epidural stimulation restores arterial pressure regulation during orthostasis. J Appl Physiol 2004 ; 97 : 984.
9) Guyton AC, Coleman TG, Granger HJ. Circulation : overall regulation. Ann Rev Physiol 1972 ; 34 : 13.
10) Sato T, Kawada T, Inagaki M, et al. New analytic

framework for understanding sympathetic baroreflex control of arterial pressure. Am J Physiol Heart Circ Physiol 1999 ; 276 : H2251.

11) Sunagawa K, Sato T, Kawada T. Integrative sympathetic baroreflex regulation of arterial pressure. Ann NY Acad Sci 2001 ; 940 : 314.

12) Kawada K, Sunagawa G, Takaki H, et al. Development of a servo-controller of heart rate using a treadmill. Jpn Circ J 1999 ; 63 : 945.

13) Hainsworth R, Karim F. Responses of abdominal vascular capacitance in the anaesthetized dog to changes in carotid sinus pressure. J Physiol (Lond) 1976 ; 262 : 659.

14) Carneiro JJ, Donald DE. Blood reservoir function of dog spleen, liver, and intestine. Am J Physiol Heart Circ Physiol 1977 ; 232 : H67.

15) Minson CT, Wladkowski SL, Pawelczyk JA, et al. Age, splanchnic vasoconstriction, and heat stress during tilting. Am J Physiol Regul Integr Comp Physiol 1999 ; 276 : R203.

16) Kahn RL, Marino V, Urquhart B, et al. Hemodynamic changes associated with tourniquet use under epidural anesthesia for total knee arthroplasty. Reg Anesth 1992 ; 17 : 228.

17) Sander-Jensen K, Mehlsen J, Secher NH, et al. Progressive central hypovolaemia in man–resulting in a vasovagal syncope? Haemodynamic and endocrine variables during venous tourniquets of the thighs. Clin Physiol 1987 ; 7 : 231.

18) Reid SA. Surgical technique for implantation of the neurocybernetic prosthesis. Epilepsia 1990 ; 31 Suppl 2 : S38.

* * *

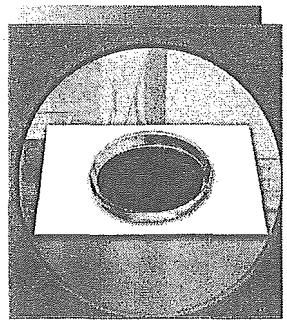

Bionic Cardiovascular Medicine

Functional Replacement of Native Cardiovascular Regulation and the Correction of Its Abnormality

BY MASARU SUGIMACHI
AND KENJI SUNAGAWA

We have developed a novel, bionic therapeutic strategy to treat various incurable cardiovascular diseases. The bionic therapeutic strategy comprises a collection of methods to treat various diseases by replacing the native regulatory function or by correcting the abnormal native function with intelligent electronic devices. We have succeeded in decoding the heart rate from the sympathetic nervous system, encoding pressor information and delivering it via nervous stimulation sequence, and improving the survival of animals with chronic heart failure by the correction of the abnormal cardiovascular regulatory function.

Bionic Cardiovascular Medicine

The term *bionic therapeutic strategy* denotes a collection of methods used to treat various diseases by replacing the native regulatory system with intelligent electronic devices [Figure 1(a)]. This strategy allows treatment of various cardiovascular diseases by compensating the deficiencies of the native cardiovascular regulatory system caused by diseases. If the electronic device can mimic native regulatory function, then it can also regulate the cardiovascular system and operate as if it were the native system. To achieve this goal, one has to interface the device with the autonomic nervous system. Depending on whether the neural interface is on the afferent or efferent side of the device, the device is able to either listen to the voices of the autonomic nerves or drive the autonomic nerves to execute appropriate cardiovascular control.

In one of our studies, we have tried to decipher the message from the brain by decoding the efferent neural activities. In our specific study detailed in the following, this approach effectively replaces the neural control of heart rate. This framework proved useful in the development of a neural-regulated cardiac pacemaker [1]. The pacemaker is able to adjust the heart rate as if it were regulated by the native sympathetic nervous system.

In another study, we have developed techniques to drive the autonomic nervous system by encoding information for cardiovascular control and delivering it via the neural stimulation sequence. This allows us to replace part of the medullary regulatory function; in other words, to create the brain function. Using this framework, we were able to replace the medullary vasomotor center and restore the normal pressure-stabilizing function of the brain [2], [3].

In yet another study, the bionic therapeutic strategy was able to correct the abnormal regulatory function accompanying some diseases [Figure 1(b)]. This correction proved to be effective in improving the survival of animals with chronic heart failure [4]. We have also demonstrated that altering native function rather than mimicking it has beneficial effects on survival in chronic heart failure. In this case, the electronic device can augment brain function.

Functional Identification of the Cardiovascular System: White-Noise Method

Replacement of lost native function or correction of abnormal native function requires comprehensive identification of the normal cardiovascular regulatory system. For this purpose, we used the white-noise method, where white noise was imposed as the input to the system to be identified. The wideband nature of white-noise input allows estimation of the wideband system dynamic properties. In addition, we ensemble-averaged the input power and cross power to reduce the statistical variance [5]–[7].

As shown in Figure 2, both input, $x(t)$, and output, $y(t)$, signals are divided into multiple segments. These data are subjected to frequency analysis using a fast Fourier transform (FFT) algorithm, $X(f)$ and $Y(f)$. The calculated input power and cross power (between input and output signals) are ensemble-averaged across segments to reduce variance, $XX(f)$ and $YX(f)$. Finally, the transfer function $H(f)$ is obtained by dividing the ensembled cross power by the ensembled input power. The impulse response $h(t)$ is calculated by the inverse FFT of the transfer function.

Deciphering the Message from the Brain: Development of a Neural-Regulated Pacemaker

The cardiac pacemaker is an established device used to treat bradyarrhythmias. Development of the dual-chamber (DDD) pacemaker has improved the coordination between the electrical activity of the atria and ventricles. In patients with preserved atrial function, a DDD pacemaker allows changes in heart rate in response to exercise as well as psychological excitation. To treat patients who have lost atrial function, it is

 0739-5175/05/$20.00©2005IEEE

necessary to stimulate the atrium in a physiological manner. For this purpose, the rate-responsive (DDDR) pacemaker has been developed [8]. The DDDR pacemaker is designed to change heart rates in response to changes such as body temperature, acceleration, and electrocardiographic QT interval. Even with the rate-responsive pacemaker, however, the heart rate responses are still not quite physiological.

In animals and humans, heart rate is regulated by the autonomic (sympathetic and vagal) nervous system [9]–[11]. Since information on the true physiological target of heart rate control is contained within the autonomic nervous activity; deriving heart rate changes continuously from analysis of neural activity has made it possible to develop a truly physiological pacemaker; the neural-regulated pacemaker (Figure 3). In other words, the message from the brain can be deciphered by decoding the heart rate information from the efferent neural traffic. A neural-regulated pacemaker is then able to adjust heart rate as if it were regulated by the native sympathetic nervous system.

Figure 4 illustrates an example of our attempt to decode heart rate information from sympathetic nervous activity. We first examined the instantaneous relationship between nervous activity and heart rate [see time course Figure 4(a)]. A scatter plot of these two variables [Figure 4(c)] seems to show that they are not at all related.

To further investigate the relationship between nervous activity and heart rate, we identified the transfer function and the impulse response of the system. The results indicate that heart rate is dependent on not only the instantaneous nervous activity but also its history (Figure 5). Specifically, the impulse response $h(k)$ quantifies the effect of past nervous activity $NA(n-k)$ on heart rate $HR(n)$ at a point in time n.

Figure 4(b) provides an example of how the impulse response is used successfully to decode heart rate from current and past nervous activities. The estimated changes in heart

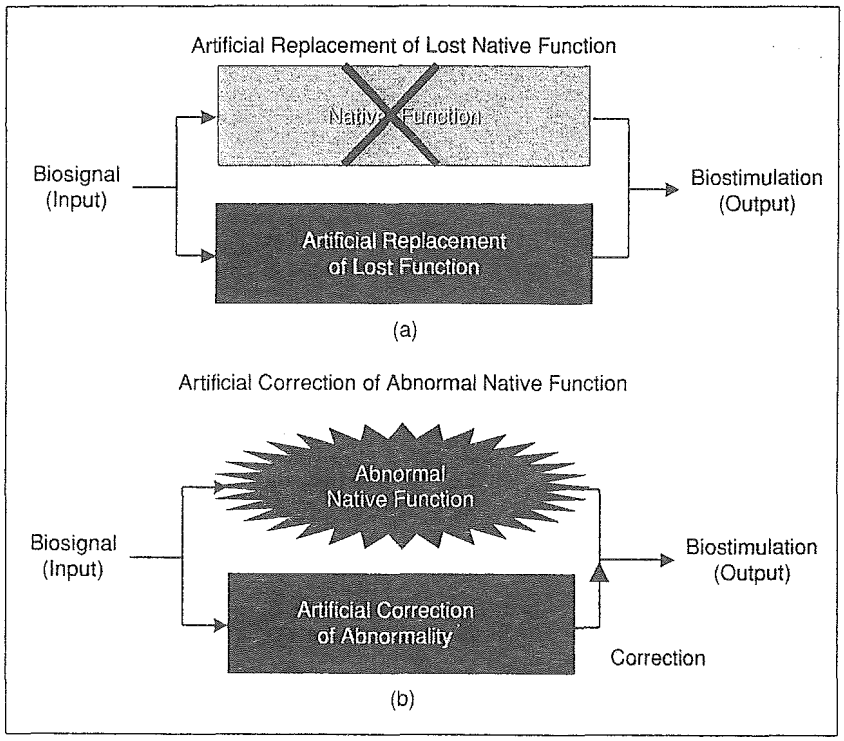

Fig. 1. Bionic medicine either replaces the lost native function or corrects the abnormal native function with the use of artificial devices.

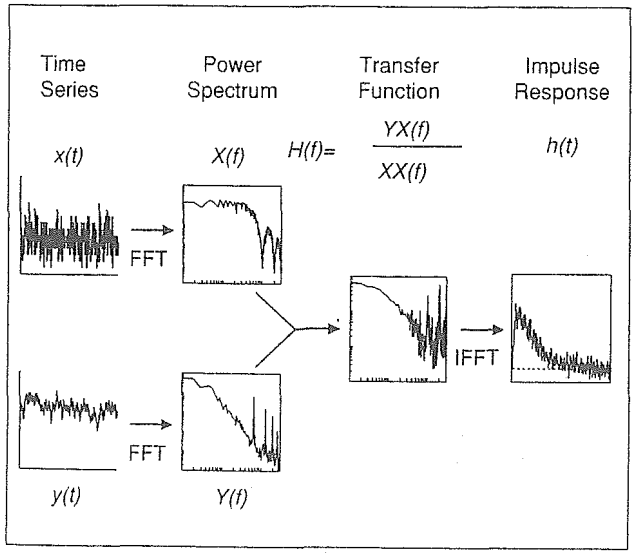

Fig. 2. Functional identification of the native regulatory system with the white-noise method. Transfer function and impulse response describe the comprehensive dynamic properties: *x(t)*, input; *y(t)*, output; *X(f)*, input spectrum; *Y(f)*, output spectrum; *XX(f)*, input power; *YX(f)*, cross power; *H(f)*, transfer function; *h(t)*, impulse response.

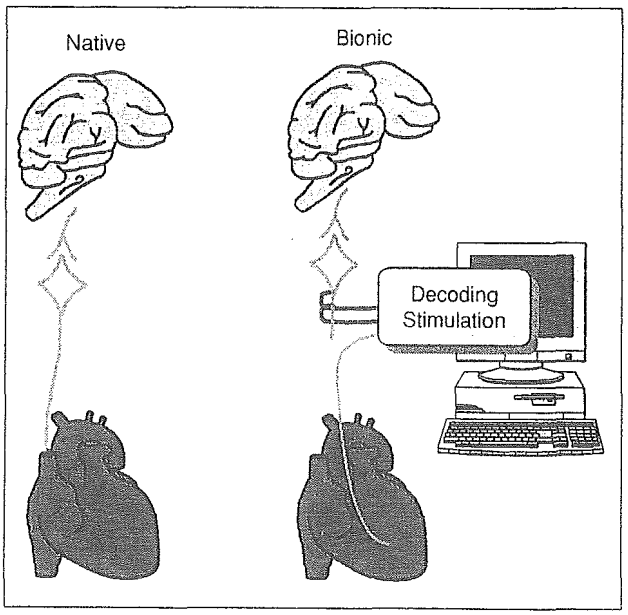

Fig. 3. Schematic presentation of the bionic (neural-regulated) pacemaker. By deciphering the message from the brain (decoding from the neural activity), one can reproduce the truly physiological changes in heart rate.

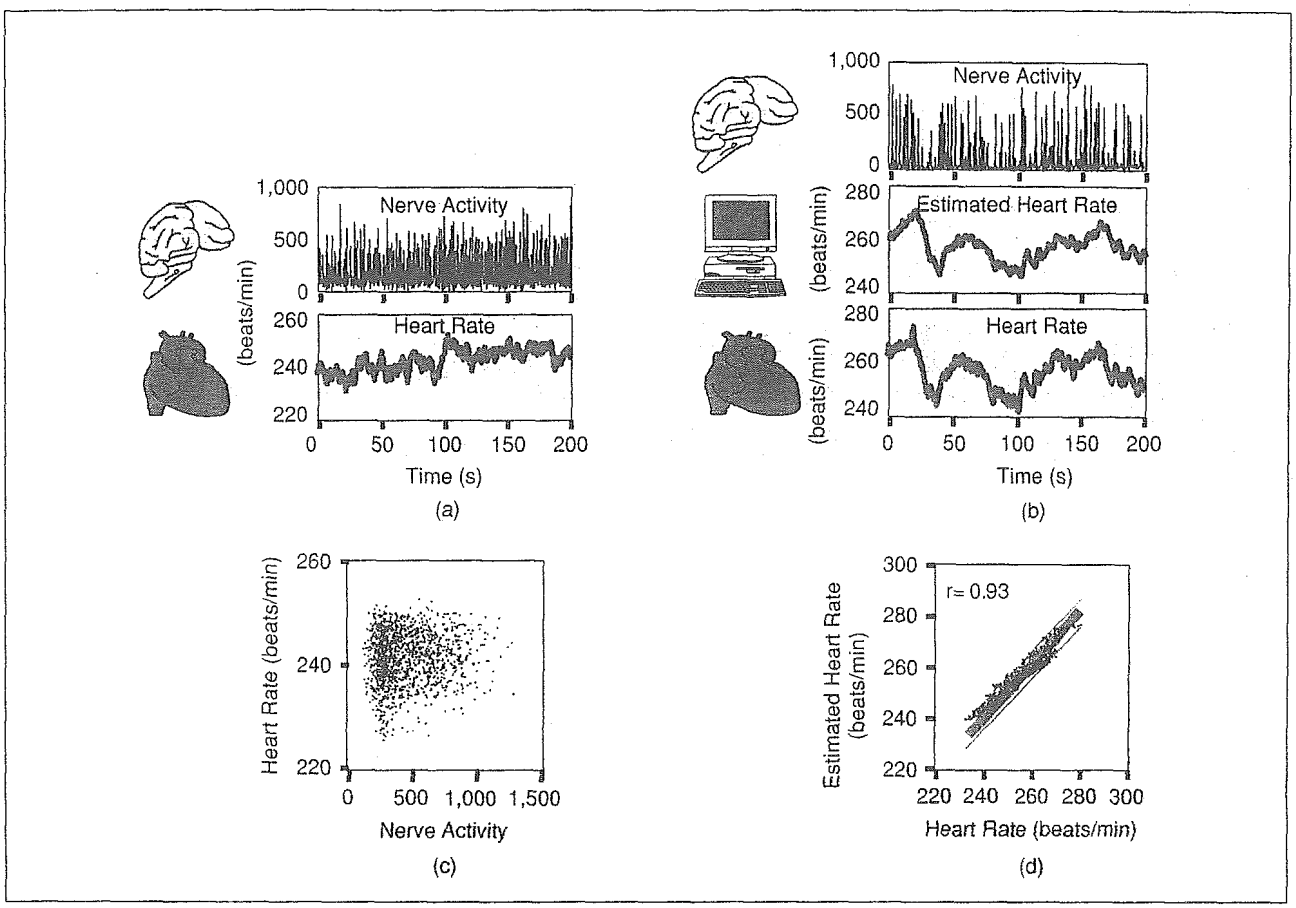

Fig. 4. An example showing how the decoding improves the estimation accuracy of the physiological changes in heart rate (modified from (1)).

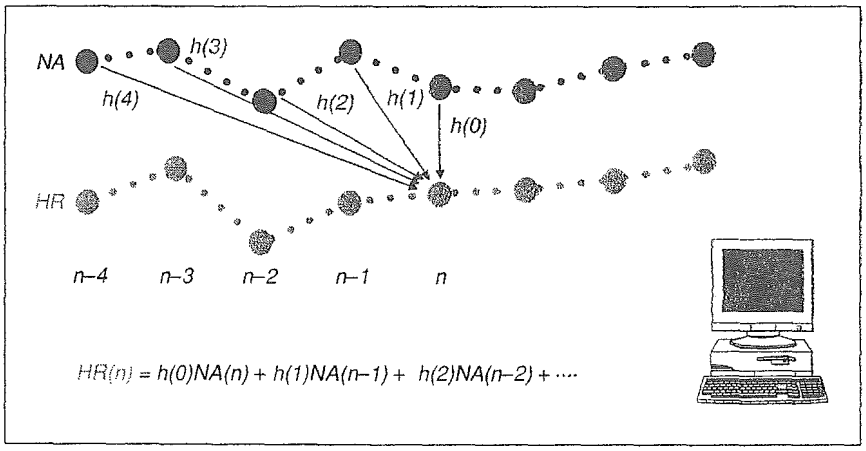

Fig. 5. Heart rate is determined not only by the instantaneous nervous activity, but also by its history. The impulse response, *h(k)*, represents how each past neural activity, *NA(n-k)*, affects the heart rate, *HR(n)*.

rate (time course) are shown to almost superimpose the measured changes [Figure 4(b)]. The accuracy of the estimation is further demonstrated by the scatter plot [Figure 4(d)]. In this particular example, the correlation coefficient was 0.93.

Accurate estimation of heart rate has also been achieved in other animals [1]. In eight anesthetized rabbits, the transfer function was approximated by a first-order, low-pass filter (corner frequency, 0.024 ± 0.013 Hz) with a lag time of 0.98 ± 0.09 s. The estimated heart rate correlated well with the measured heart rate, with correlation coefficients between 0.80 and 0.98. The standard error of the prediction was 1.2 ± 0.7% of the average heart rate examined, indicating that the heart rate estimation is sufficiently accurate for use in cardiac pacing. Thus, decoding instantaneous heart rate from sympathetic nervous activity is possible via impulse response analysis. This framework enables the development of a neural-regulated artificial pacemaker with a truly physiological heart rate control.

Creating the Brain: Development of Artificial Vasomotor Center

It is well known that animals and humans are equipped with baroreceptors (pressure sensors) in the walls of the carotid sinus and aortic arch. Information from these baroreceptors is used to stabilize blood pressure and maintain the homeostasis of the body. This pressure stabilizing system forms a negative feedback system, which is called the arterial baroreflex system. A decrease in blood pressure induces a pressor command at the vasomotor center located in the medulla. The pressor command increases pressure through a positive inotropic and chronotropic effect on the heart, and a vasoconstrictive effect on the blood vessels [12].

Patients lacking a functional vasomotor center in the brain suffer from severe orthostatic hypotension, and are often confined to bed [13]. They include patients with spinal cord injury and central degenerative diseases such as Shy-Drager syndrome. These patients lose consciousness during sitting and standing due to the severe hypotension attending these conditions, despite normal functions of the cardiovascular system and peripheral sympathetic nervous system. In fact, these patients suffer from hypertension in the supine position.

Blood pressure can be measured with artificial manometers (pressure sensors) such as semiconductor sensors. By feeding the blood pressure information into an electronic device that substitutes the nonfunctioning native vasomotor center, it is possible to drive the sympathetic nervous system (Figure 6). If the sympathetic nerve is appropriately stimulated to provide a sufficiently quick and stable feedback system, then the pressure-stabilizing function of the arterial baroreflex system can be restored.

One of the methods to achieve appropriate stimulation is to mimic the function of the native vasomotor center. If the mechanism of how the native vasomotor center drives the sympathetic nervous system in response to pressure changes is elucidated, then the feedback loop may be closed with sufficient speed and stability [14]–[17]. Since this treatment framework involves replacing a part of the brain function with an artificial device, it is called bionic treatment with electronic creation of brain function.

We first examined experimentally whether restoration of vasomotor center function is possible in anesthetized rats. We placed a catheter-tipped micromanometer in the aortic arch and implanted stimulation electrodes on the greater splanchnic nerve (celiac ganglion).

The encoding rule for the bionic brain (artificial vasomotor center) was determined by a white-noise approach in the following manner (Figure 7). We first estimated the open-loop dynamic properties of the native total baroreflex system. The dynamic properties, i.e., the transfer function (H_{NATIVE}), were obtained by analyzing the dynamic relationships between carotid sinus pressure (input) and blood pressure (output) after carotid sinus isolation and aortic denervation. We then determined the dynamic response of blood pressure (AoP) to electrical stimulation (STM) of the celiac ganglion ($H_{STM \rightarrow AoP}$: effector response). To match the dynamic properties of the total baroreflex response with the serially connected bionic brain and the effector response, we computed the dynamic property (encoding rule, H_{BIONIC}) of the bionic brain by $H_{NATIVE}/H_{STM \rightarrow AoP}$ and entered the encoding rule into the computer. The open-loop transfer function of the artificial vasomotor center was identified as a high-pass filter with a corner frequency of 0.1 Hz [2], [3], [18].

Figure 8 depicts an example of how functional replacement of the vasomotor center with the bionic brain restores the pressure stabilization after head-up tilt tests. The rat was subjected to a constant baroreflex input by carotid sinus isolation and aortic denervation. This procedure produced a "baroreflex failure" rat.

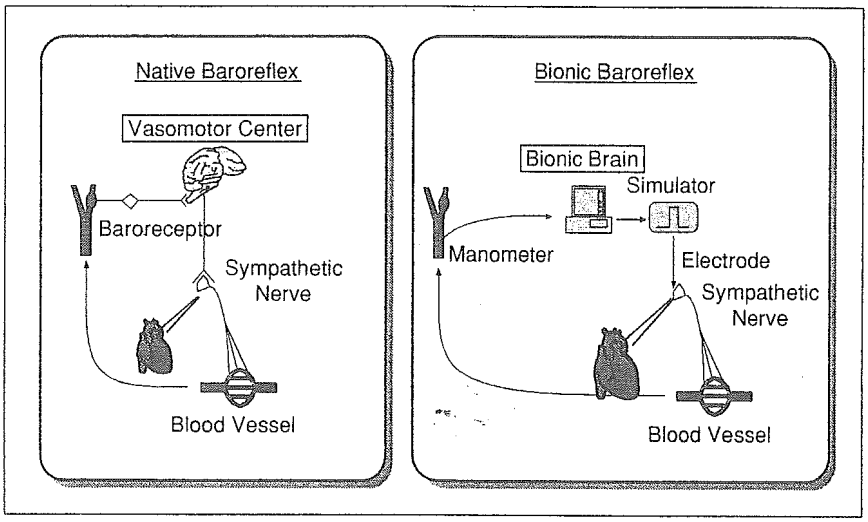

Fig. 6. Schematic presentation of the bionic baroreflex. The bionic brain (artificial vasomotor center) drives the sympathetic nerves in response to pressure perturbation. The encoding rule was obtained by mimicking the native vasomotor center. The bionic brain functionally replaces the vasomotor center, artificially creating the brain function (modified from (2)).

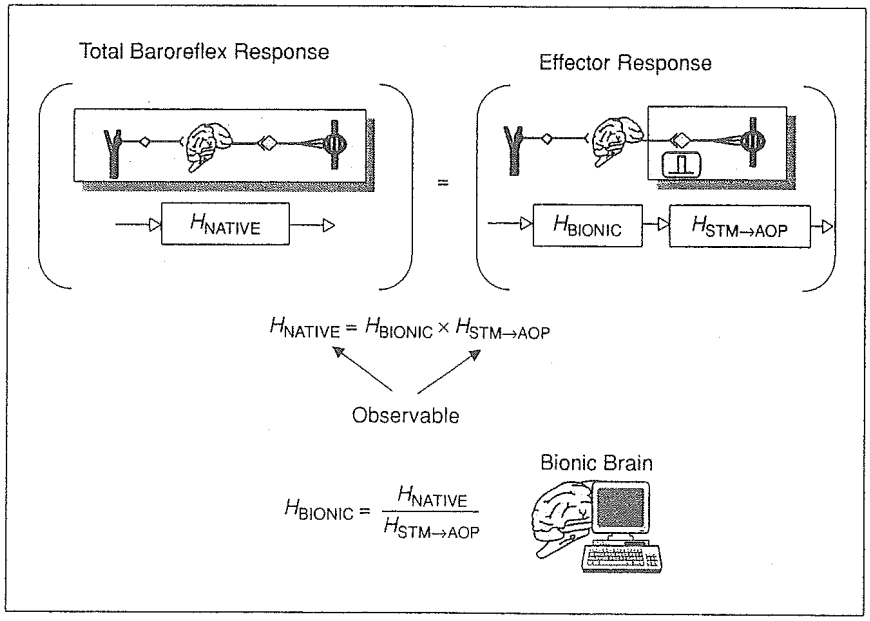

Fig. 7. Method to identify the dynamic properties of the bionic brain. H_{NATIVE}, total baroreflex properties; H_{BIONIC}, bionic brain (artificial vasomotor center) properties; $H_{STM \rightarrow AoP}$, effector properties; *STM*, electrical stimulation frequency; *AoP*, blood pressure (modified from (2)).

If the electronic device can mimic native regulatory function, then it can also regulate the cardiovascular system and operate as if it were the native system.

In a rat with normal baroreflex, a 90° head-up tilt decreases blood pressure by approximately 10 mmHg. When the "baroreflex failure" rat was tested, the head-up tilt drastically decreased blood pressure by approximately 50 mmHg. By activating the bionic baroreflex in the "baroreflex failure" rat, blood pressure did not decrease more than 10 mmHg.

Pressure stabilization provided by the bionic brain was verified in other experiments using rats [2], [3]. The pressure stabilization process was examined by two approaches. First, we evaluated the performance of the bionic brain in response to sudden local imposition of a pressure step on carotid sinus baroreceptors in 16 anesthetized rats [2]. Without the bionic brain, blood pressure fell rapidly by 49 ± 8 mmHg in 10 s. With the bionic brain online in real-time execution mode, blood pressure fell only by 22 ± 6 mmHg at the nadir and by 16 ± 5 mmHg at the plateau. These pressure changes were statistically indistinguishable from those of the native baroreflex system.

In ten other rats with baroreflex failure, we evaluated the performance of the bionic brain by the 90° head-up tilt tests [3]. Abrupt head-up tilt decreased blood pressure by 34 ± 6 mmHg in 2 s and by 52 ± 5 mmHg in 10 s. With real-time execution of the bionic brain, the pressure fall was only 21 ± 5 mmHg at 2 s and 15 ± 6 mmHg at 10 s after starting the head-up tilt. The pressure responses observed with the bionic brain in action were indistinguishable from those observed with a normal native baroreflex system.

From these data, we conclude that the bionic brain is able to restore the native baroreflex function in rats with baroreflex failure. Development of appropriate long-term manometry and an implantable neural stimulation system would provide a novel modality to treat incurable bed-ridden conditions such as Shy-Drager syndrome.

Surpassing the Native Brain: Bionic Treatment of Chronic Heart Failure

Bionic treatment so far, described as "deciphering the message of the brain" and "creating the brain function," operates by replacing the lost native function with artificial electronic devices. These devices operate as if they were native regulatory systems. However, in some pathological states, the native regulatory system acts in a detrimental fashion against recovery from the disease. Heart failure is perhaps the most well-known disease in which the native regulatory system is essential for the maintenance and progression of the disease [19]. In heart failure, there is a possibility that correction of the abnormal regulatory function may inhibit or slow the progression of the disease. If this treatment proves effective, it will open a possibility of yet another type of bionic treatment, which we designate "surpassing the native brain function." In earlier studies, diminished cardiac vagal activity and higher heart rate predict a high mortality of heart failure [20]. Previous megatrials in patients with heart failure have demonstrated that drugs stimulating cardiovascular function aggravate long-term survival, whereas those inhibiting cardiovascular function improve survival. Based on these studies, we hypothesize that stimulating vagal activity using a bionic negative feedback control system decreases mortality.

To examine this hypothesis, we conducted experiments in rats with severe heart failure. Hemodynamics

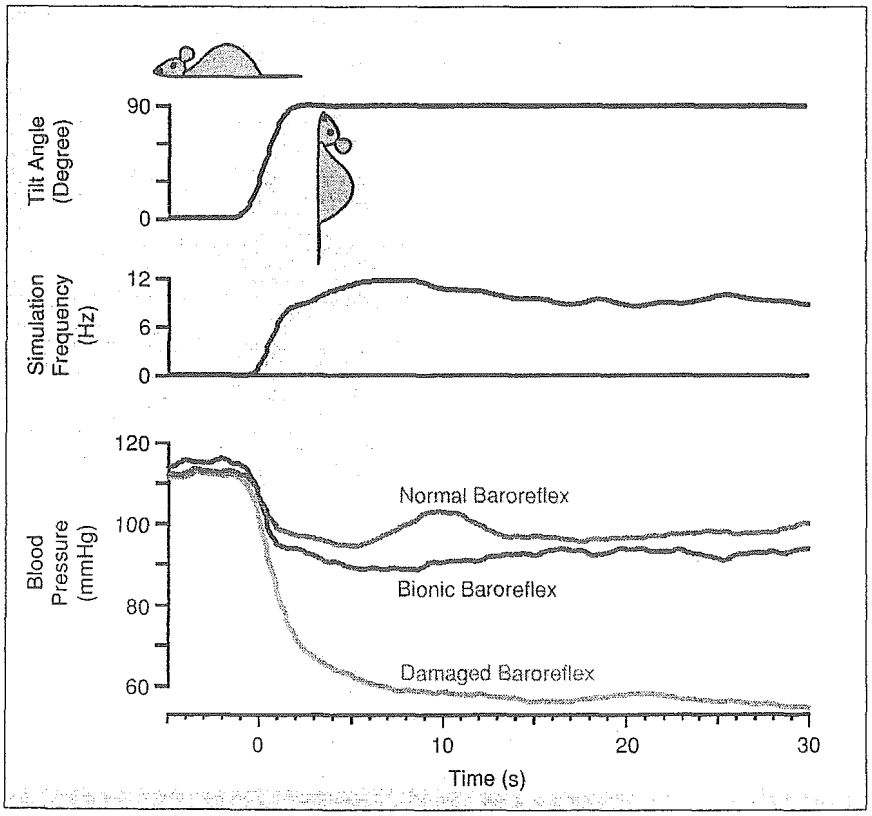

Fig. 8. An example that illustrates how the activation of the bionic brain improves pressure stabilization; it prevents orthostatic hypotension (modified from (3)).

Replacement of lost native function or correction of abnormal native function requires comprehensive identification of the normal cardiovascular regulatory system.

and remodeling were examined in 26 rats, while survival was examined in 52 rats.

In eight-week-old male Sprague-Dawley (SD) rats anesthetized with 1% halothane, the chest was opened and the left coronary artery was ligated at 2–3 mm from its origin. The coronary ligation procedure produced a large myocardial infarct (40–50%), followed by remodeling of the heart and eventually severe heart failure. Since these rats were highly susceptible to ventricular fibrillation, we used mechanical defibrillation by cardiac massage if necessary. If the animal survived the acute period, the chest was closed and the animal was allowed to recover.

After one week, surviving rats were randomized to two groups: a bionic treatment group with vagal stimulation and a control group. These animals underwent another surgery under halothane anesthesia. In the bionic treatment group, we isolated the right cervical vagus nerve and attached a bipolar electrode to be used for telestimulation. We also implanted two devices: a miniature radio-controlled electrical stimulator (telestimulation device) and a blood pressure telemetric device for heart rate monitoring. In the control group, we only isolated the right cervical vagus nerve without implanting any device.

One week after the second surgery, the surviving rats in the bionic treatment group received right vagal stimulation to achieve a target reduction in heart rate (Figure 9). Vagal stimulation was continued for six weeks (two to eight weeks after coronary ligation), with the target heart rate set at 10–20% (20–30 beats/min) lower than the control. The stimulation consisted of a current pulse with an amplitude of 0.1–0.13 mA, pulse width of 0.2 ms, and repetition frequency of 20 Hz. Vagal stimulation was delivered intermittently, for 10 s/min.

At six weeks, vagal stimulation was terminated, and hemodynamic and echocardiographic measurements were obtained under halothane anesthesia. Hemodynamics were obtained using a 2-Fr catheter tipped micromanometer inserted via an apical stab wound. The animals were sacrificed, and the heart weights were measured.

To examine survival, the animals were observed for 14 weeks after vagal stimulation was terminated, a total of 20 weeks (140 days) of observation.

Hemodynamics were examined in 12 rats from the bionic treatment group and 14 rats from the control group [Figure 10(a)]. Infarct size was quantified by histological examination of the ratio of the infarct area to the short-axis cross-sectional area of myocardium. No significant difference in infarct size was observed between the two groups (46 ± 9% in the bionic treatment group, 43 ± 10% in the control group). Heart weight (normalized by body weight, *HW/BW*) was significantly lower in the bionic treatment group (2.71 ± 0.24 g/Kg, $p < 0.05$) than in the control group (3.01 ± 0.31 g/Kg), indicating that cardiac remodeling was inhibited by the bionic treatment with vagal stimulation. The ratio of inhibition in heart weight increase was equivalent to the amount observed in rats receiving angiotensin-converting enzyme inhibitors. Left ventricular contractility was evaluated by the maximal first derivative of left ventricular pressure ($LV + dP/dt$ max). This index was significantly larger (4,206 ± 244 mmHg/s, $p < 0.001$) in the bionic treatment group than in the control group (2,999 ± 173 mmHg/s), indicating preserved function of the noninfarct myocardium. Left ventricular filling pressure (left ventricular end-diastolic pressure, LVEDP) tended to be lower (17 ± 6 mmHg versus 23 ± 5 mmHg) and echocardiographically determined fractional shortening of the left ventricle tended to be larger (15 ± 4%

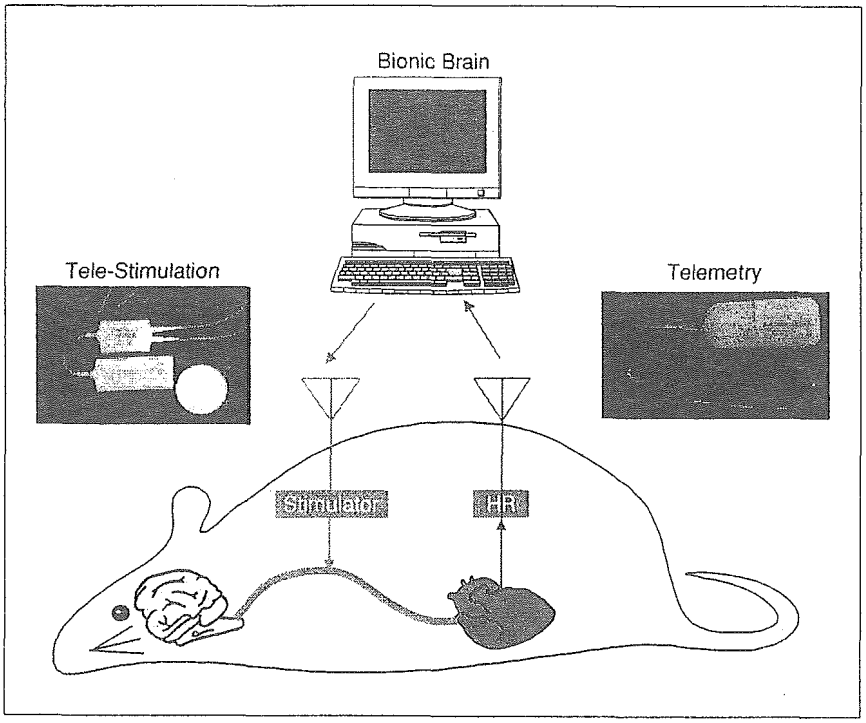

Fig. 9. Animal preparation to depict the bionic treatment of heart failure with vagal stimulation. Heart rate (HR) was continuously monitored by the pressure telemetry while vagal stimulation was delivered by the telestimulation.

One of the methods to achieve appropriate stimulation is to mimic the function of the native vasomotor center.

versus 11 ± 3%) in the bionic treatment group.

Survival was examined in 22 rats in the bionic treatment group and 30 rats in the control group [Figure 10(b)] [4]. While the 20-week survival of the untreated group was only 50%, a markedly improved survival rate (86%, $p = 0.008$) was observed in the bionic treatment group with vagal stimulation. The bionic treatment achieved a 73% reduction in a relative risk of death. The degree of reduction in the relative risk by the bionic treatment far exceeded those by the conventional therapy with drugs such as angiotensin-converting enzyme inhibitors, beta-adrenergic blockers, and spironolactones. The improved survival persisted for 20 weeks, even though the bionic treatment was stopped at six weeks.

These data indicate that the bionic treatment with vagal nerve stimulation markedly improves the long-term survival of rats with heart failure through preventing pumping failure and cardiac remodeling.

The Potential and the Future of Bionic Medicine

We have demonstrated that the bionic cardiovascular medicine permits both the replacement of lost native function and the correction of the abnormal native function. These results demonstrate the efficacy of the new treatment framework, particularly for various incurable diseases.

These results indicate the importance of the regulatory system in the maintenance and progression of various cardiovascular diseases. Furthermore, the success of bionic medicine opens up a new treatment strategy that might be called *functional reconstruction*. This is in stark contrast with the conventional treatment strategy, namely, the etiology-oriented treatment. Since efforts to identify the true cause of a disease often fail, and the cause, even if identified, may not be removable, the new treatment strategy of functional reconstruction serves as a useful alternative modality to combat various incurable diseases.

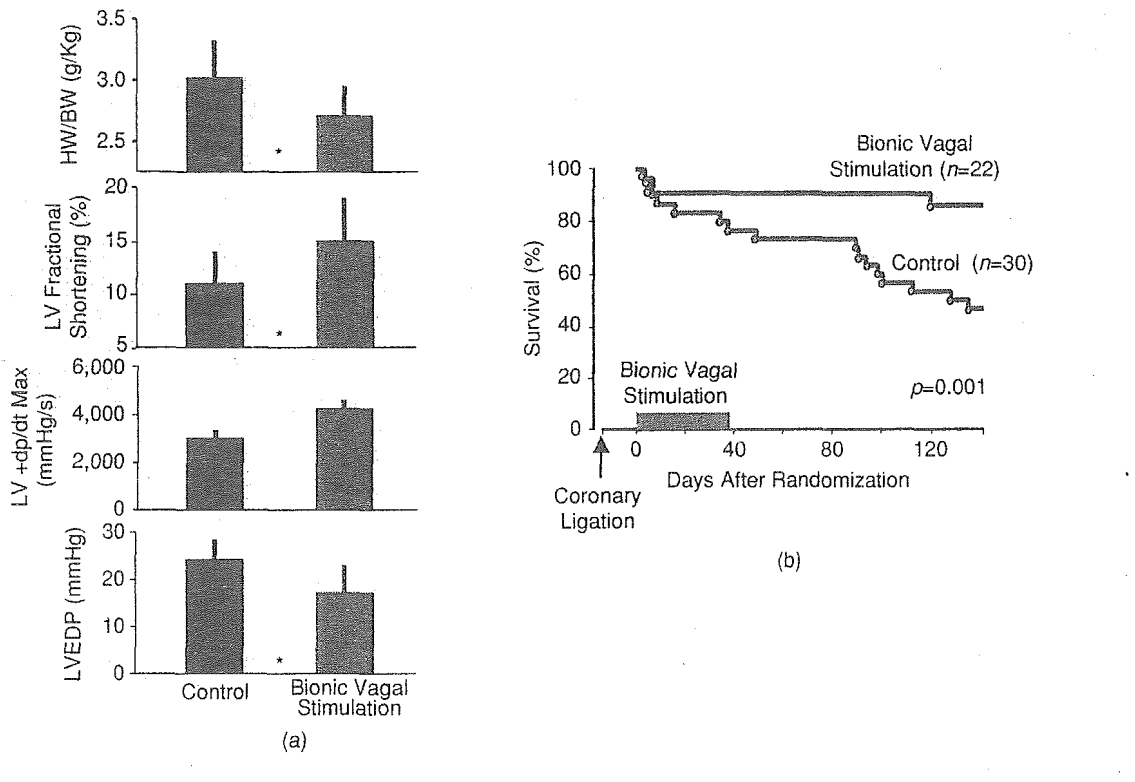

Fig. 10. Long-term bionic treatment of heart failure prevented cardiac remodeling and pumping failure and improved survival. HW, heart weight; BW, body weight; LV, left ventricular; +dP/dt max, maximal first derivative of pressure; EDP, end-diastolic pressure (modified from (4)).

Long-term continuous treatment (manipulation or modification of cardiovascular function) by means of implantable electronics is quite feasible. The measurement of biosignals and the electrical stimulation of biological tissue can be achieved using low-power electronic circuits. Implantation of devices with appropriate treatment logic and close patient monitoring with wireless telecommunication would greatly enhance the therapeutic effects during daily life outside the hospital. At the same time, continuous treatment would reduce the rate of hospital visits and save resources for the medical service.

Finally, the bionic treatment reduces the mortality of rats with heart failure to an extent not achieved by popular cardiovascular drugs. It also appears to be useful in inhibiting fatal cardiac arrhythmias. Based on these findings, the bionic treatment is a most promising approach in improving survival as well as the quality of life of patients with life-threatening cardiovascular diseases.

Acknowledgments

This study was supported by the Health and Labour Sciences Research Grant for Research on Advanced Medical Technology (H14-nano-002) and for Analyzing, Supporting, and Substituting the Function of Human Body (H15-physi-001) from the Ministry of Health Labour and Welfare of Japan and the Program for Promotion of Fundamental Studies in Health Science of the Organization for Pharmaceutical Safety and Research of Japan.

Masaru Sugimachi is the director of the Department of Cardiovascular Dynamics, National Cardiovascular Center Research Institute, Osaka, Japan. He received his M.D. in 1984 from Kyushu University, Japan, and his Ph.D. in biomedical engineering from Kyushu University in 1992. From 1992–2004, he was at the Department of Cardiovascular Dynamics, the National Cardiovascular Center, Osaka, where he integrated the research team for the clinical application of bionic cardiology. He has published more than 100 original papers in cardiac mechanics, cardiovascular regulation, modeling of biological systems, and bionic medicine. He is currently the principal investigator of four major national research projects where he has been developing intelligent implantable cardiac autonomic neuroregulators to treat heart failure, distributed micropacemakers, a next generation implantable cardioverter defribrillator (ICD), and an intensive cardiac care autopilot system.

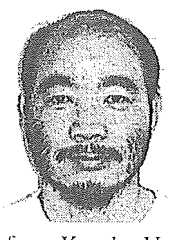

Kenji Sunagawa is the chair and professor of the Department of Cardiovascular Medicine, Graduate School of Medical Sciences, Kyushu University, Fukuoka, Japan. He has been a member of the administrative committee of the Japanese Society of Medical Electronics and Biological Engineering. He received his M.D. in 1974 from Kyushu University and his Ph.D. in biomedical engineering from Kyushu University in 1985. In 1978, he joined the Department of Biomedical Engineering at Johns Hopkins Medical School where he established the concept of ventricular-arterial coupling. The coupling concept has been adopted for many textbooks of cardiology and cardiac physiology worldwide. From 1992–2004, he chaired the Department of Cardiovascular Dynamics at the National Cardiovascular Center, Osaka, Japan, and developed the basis of bionic cardiology.

Address for Correspondence: Masaru Sugimachi M.D., Ph.D., Department of Cardiovascular Dynamics, National Cardiovascular Center Research Institute 5-7-1 Fujishirodai, Suita, Osaka 565-8565 Japan. Phone: +81 6 6833 5012. Fax: +81 6 6835 5403. E-mail: sugimach@ri.ncvc.go.jp.

References

[1] Y. Ikeda, M. Sugimachi, T. Yamasaki, O. Kawaguchi, T. Shishido, T. Kawada, J. Alexander, Jr., and K. Sunagawa, "Explorations into development of a neurally regulated cardiac pacemaker," *Amer. J. Physiol.*, vol. 269, no. 6, pp. H2141–H2146, Dec. 1995.

[2] T. Sato, T. Kawada, T. Shishido, M. Sugimachi, J. Alexander, Jr., and K. Sunagawa, "Novel therapeutic strategy against central baroreflex failure: A bionic baroreflex system," *Circulation*, vol. 100, no. 3, pp. 299–304, Jul. 1999.

[3] T. Sato, T. Kawada, M. Sugimachi, and K. Sunagawa, "Bionic technology revitalizes native baroreflex function in rats with baroreflex failure," *Circulation*, vol. 106, no. 6, pp. 730–734, Aug. 2002.

[4] M. Li, C. Zheng, T. Sato, T. Kawada, M. Sugimachi, and K. Sunagawa, "Vagal nerve stimulation markedly improves long-term survival after chronic heart failure in rats," *Circulation*, vol. 109, no. 1, pp. 120–124, Jan. 2004.

[5] P.Z. Marmarelis and V.Z. Marmarelis, *Analysis of Physiological Systems: The White-Noise Approach*. New York: Plenum, 1978.

[6] J.S. Bendat and A.G. Piersol, *Random Data: Analysis and Measurement Procedures*, 3rd ed. New York: Wiley-Interscience, 2000.

[7] M. Sugimachi, T. Imaizumi, K. Sunagawa, Y. Hirooka, K. Todaka, A. Takeshita, and M. Nakamura, "A new method to identify dynamic transduction properties of aortic baroreceptors," *Amer. J. Physiol.*, vol. 258, no. 3, pp. H887–H895, Mar. 1990.

[8] K. Jeffrey, "The next step in cardiac pacing: the view from 1958," *Pacing Clin. Electrophysiol.*, vol. 15, no. 6, pp. 961–967, June 1992.

[9] T. Kawada, Y. Ikeda, M. Sugimachi, T. Shishido, O. Kawaguchi, T. Yamazaki, J. Alexander, Jr., and K. Sunagawa, "Bidirectional augmentation of heart rate regulation by autonomic nervous system in rabbits," *Amer. J. Physiol.*, vol. 271, no. 1, pp. H288–H295, Jul. 1996.

[10] T. Kawada, M. Sugimachi, T. Shishido, H. Miyano, Y. Ikeda, R. Yoshimura, T. Sato, H. Takaki, J. Alexander, Jr., and K. Sunagawa, "Dynamic vagosympathetic interaction augments heart rate response irrespective of stimulation patterns," *Amer. J. Physiol.*, vol. 272, no. 5, pp. H2180–H2187, May 1997.

[11] T. Kawada, M. Sugimachi, T. Shishido, H. Miyano, T. Sato, R. Yoshimura, H. Miyashita, T. Nakahara, J. Alexander, Jr., and K. Sunagawa, "Simultaneous identification of static and dynamic vagosympathetic interactions in regulating heart rate," *Amer. J. Physiol.*, vol. 276, no. 3, pp. R782–R789, Mar. 1999.

[12] A.C. Guyton, T.G. Coleman, and H.J. Granger, "Circulation: Overall regulation," *Annu. Rev. Physiol.*, vol. 34, pp. 13–46, Mar. 1972.

[13] Consensus Committee of the American Autonomic Society and the American Academy of Neurology, "Consensus statement on the definition of orthostatic hypotension, pure autonomic failure, and multiple system atrophy," *Neurology*, vol. 46, no. 5, p. 1470, May 1996.

[14] Y. Ikeda, T. Kawada, M. Sugimachi, O. Kawaguchi, T. Shishido, T. Sato, H. Miyano, W. Matsuura, J. Alexander, Jr., and K. Sunagawa, "Neural arc of baroreflex optimizes dynamic pressure regulation in achieving both stability and quickness," *Amer. J. Physiol.*, vol. 271, pp. H882–H890, Sept. 1996.

[15] K. Sunagawa, Y. Ikeda, T. Kawada, M. Sugimachi, T. Shishido, T. Sato, H. Miyano, W. Matsuura, M. Inagaki, and J. Alexander, Jr., "Dynamic control of arterial blood pressure by the sympathetic baroreflex," *Fundam. Clin. Pharmacol.*, vol. 12, suppl. 1, pp. 23s–28s, June 1998.

[16] T. Sato, T. Kawada, M. Inagaki, T. Shishido, M. Sugimachi, and K. Sunagawa, "Dynamics of sympathetic baroreflex control of arterial pressure in rats," *Amer. J. Physiol. Regul. Integr. Comp. Physiol.*, vol. 285, no. 1, pp. R262–R270, July 2003.

[17] T. Kawada, K. Uemura, K. Kashihara, A. Kamiya, M. Sugimachi, and K. Sunagawa, "A derivative-sigmoidal model reproduces operating-point dependent baroreflex neural arc transfer characteristics," *Amer. J. Physiol. Heart Circ. Physiol.*, vol. 286, no. 6, pp. H2272–H2279, June 2004.

[18] P. Kezdi and E. Geller, "Baroreceptor control of postganglionic sympathetic nerve discharge," *Amer. J. Physiol.*, vol. 214, no. 3, pp. 427–435, Mar. 1968.

[19] M. Nagatsu, F.G. Spinale, M. Koide, H. Tagawa, G. DeFreitas, G. Cooper 4th, and B.A. Carabello, "Bradycardia and the role of beta-blockade in the amelioration of left ventricular dysfunction," *Circulation*, vol. 101, no. 6, pp. 653–659, Feb. 2000.

[20] M.T. La Rovere, J.T. Bigger, Jr., F.I. Marcus, A. Mortara, and P.J. Schwartz, "Baroreflex sensitivity and heart-rate variability in prediction of total cardiac mortality after myocardial infarction. ATRAMI (autonomic tone and reflexes after myocardial infarction) investigators," *Lancet*, vol. 351, no. 9101, pp. 478–484, Feb. 1998.

Selective disruption of MMP-2 gene exacerbates myocardial inflammation and dysfunction in mice with cytokine-induced cardiomyopathy

Hidenori Matsusaka, Masaki Ikeuchi, Shouji Matsushima, Tomomi Ide, Toru Kubota, Arthur M. Feldman, Akira Takeshita, Kenji Sunagawa and Hiroyuki Tsutsui

AJP - Heart 289:1858-1864, 2005. First published Jun 3, 2005; doi:10.1152/ajpheart.00216.2005

Am J Physiol Heart Circ Physiol 289: H1858–H1864, 2005.
First published June 3, 2005; doi:10.1152/ajpheart.00216.2005.

Selective disruption of MMP-2 gene exacerbates myocardial inflammation and dysfunction in mice with cytokine-induced cardiomyopathy

Hidenori Matsusaka,[1] Masaki Ikeuchi,[1] Shouji Matsushima,[1] Tomomi Ide,[1] Toru Kubota,[1] Arthur M. Feldman,[2] Akira Takeshita,[1] Kenji Sunagawa,[1] and Hiroyuki Tsutsui[3]

[1]*Department of Cardiovascular Medicine, Kyushu University Graduate School of Medical Sciences, Fukuoka;* [3]*Department of Cardiovascular Medicine, Hokkaido University Graduate School of Medicine, Sapporo, Japan; and* [2]*Department of Medicine, Jefferson Medical College, Philadelphia, Pennsylvania*

Submitted 7 March 2005; accepted in final form 23 May 2005

Matsusaka, Hidenori, Masaki Ikeuchi, Shouji Matsushima, Tomomi Ide, Toru Kubota, Arthur M. Feldman, Akira Takeshita, Kenji Sunagawa, and Hiroyuki Tsutsui. Selective disruption of MMP-2 gene exacerbates myocardial inflammation and dysfunction in mice with cytokine-induced cardiomyopathy. *Am J Physiol Heart Circ Physiol* 289: H1858–H1864, 2005. First published June 3, 2005; doi:10.1152/ajpheart.00216.2005.—Tumor necrosis factor-α (TNF-α) plays a pathophysiological role in the development and progression of heart failure. Matrix metalloproteinase (MMP)-2 is involved in extracellular matrix remodeling. Recent evidence suggests a protective role for this protease against tissue inflammation. Although MMP-2 is upregulated in the failing heart, little is known about its pathophysiological role. We thus hypothesized that ablation of the MMP-2 gene could affect cardiac remodeling and failure in TNF-α-induced cardiomyopathy. We crossed transgenic mice with cardiac-specific overexpression of TNF-α (TG) with MMP-2 knockout (KO) mice. Four groups of male and female mice were studied: wild-type (WT) with wild MMP-2 (WT/MMP$^{+/+}$), WT with MMP-2 KO (WT/MMP$^{-/-}$), TNF-α TG with wild MMP-2 (TG/MMP$^{+/+}$), and TG with MMP-2 KO (TG/MMP$^{-/-}$). The upregulation of MMP-2 zymographic activity in TG/MMP$^{+/+}$ mice was completely abolished in TG/MMP$^{-/-}$ mice, and other MMPs and tissue inhibitors of metalloproteinase were comparable between groups. Survival was shorter for male TG/MMP$^{-/-}$ than TG/MMP$^{+/+}$ mice. Female TG/MMP$^{-/-}$ mice were more severely affected than TG/MMP$^{+/+}$ mice with diminished cardiac function. Myocardial TNF-α and other proinflammatory cytokines were increased in TG/MMP$^{+/+}$ mice, and this increase was similarly observed in TG/MMP$^{-/-}$ mice. The extent of myocardial infiltrating cells including macrophages was greater in TG/MMP$^{-/-}$ than in TG/MMP$^{+/+}$ mice. Selective ablation of the MMP-2 gene reduces survival and exacerbates cardiac failure in association with the increased level of myocardial inflammation. MMP-2 may play a cardioprotective role in the pathogenesis of cytokine-induced cardiomyopathy.

metalloproteinases; heart failure; tumor necrosis factor

THE DYNAMIC SYNTHESIS and breakdown of extracellular matrix (ECM) proteins play an important role in myocardial remodeling and failure. In particular, increased expression and activation of matrix metalloproteinases (MMPs) have been implicated in heart failure (4, 8, 20, 23, 26, 27). The activity of MMPs is controlled by transcription, activation of the latent proenzymes, and inhibition of MMPs by tissue inhibitors of MMPs (TIMPs). Although transcriptional regulation is essential for MMP production, activation of latent enzymes by proteolytic cleavage is required for matrix degradation. In addition, TIMPs modulate ECM deposition through inhibition of activated MMPs. Together, activation of latent MMP and inhibition of MMPs by TIMPs contribute to myocardial remodeling and failure. Among the known MMPs, MMP-2 is ubiquitously distributed in cardiac myocytes and fibroblasts (2) and has been shown to be upregulated in heart failure (1, 8). Recent studies have shown that MMP-2 has diverse cellular function, such as attenuation of the tissue inflammatory response, independent of its action on the ECM (3, 13, 29). Therefore, the ultimate effects of MMPs may include modulation of ECM proteins, as well as modification of cellular functions, including cell migration.

Myocardial production of proinflammatory cytokines, including tumor necrosis factor-α (TNF-α), plays an important role in the pathogenesis of heart failure (5, 22). Transgenic (TG) mice that overexpress TNF-α specifically in the heart developed myocardial inflammation, with premature death from heart failure in association with ECM remodeling (16, 17). Activation of MMPs, i.e., MMP-2 and MMP-9, has been demonstrated in this model (17, 18). Furthermore, expression of MMP-2 can be regulated by the inflammatory cytokines (19). Therefore, MMP-2 could influence the progression of inflammation by affecting the function of mediators such as cytokines/chemokines and could play an important role in myocardial remodeling. In the present study, we evaluated the effects of a targeted deletion of the MMP-2 gene on cardiac structural and functional alterations in this type of heart failure. To ensure selective and long-term complete inhibition of MMP-2, we crossed TNF-α TG mice with MMP-2 knockout (KO) mice (8, 12). The most effective way to evaluate the contribution of a specific MMP and obtain direct evidence for a role of MMP is through gene manipulation instead of an MMP inhibitor.

MATERIALS AND METHODS

Animal model. We used TG mice with cardiac-specific overexpression of TNF-α, which have been well characterized as a model of cytokine-induced cardiomyopathy (16). To ensure complete inhibition of MMP-2 activity, we crossed TG mice with MMP-2 KO (MMP$^{-/-}$) mice. There were no detectable differences in cardiac size and structure between MMP$^{-/-}$ and MMP$^{+/+}$ mice either macroscopically or microscopically (8). The original breeding pairs used to develop the mice for this study were obtained from Dr. Shigeyoshi Itohara (Laboratory for Behavioral Genetics, RIKEN). Because

Address for reprint requests and other correspondence: H. Tsutsui, Dept. of Cardiovascular Medicine, Hokkaido Univ. Graduate School of Medicine, Kita-15, Nishi-7, Kita-ku, Sapporo 060-8638, Japan (E-mail: htsutsui@med.hokudai.ac.jp).

The costs of publication of this article were defrayed in part by the payment of page charges. The article must therefore be hereby marked "*advertisement*" in accordance with 18 U.S.C. Section 1734 solely to indicate this fact.

American Journal of Physiology - Heart and Circulatory Physiology

TNF-α TG (FVB) and MMP-2 KO (C57BL/6J) mice arise from different genetic backgrounds, we generated all mice as mixed genetic background (1:1 ratio of C57BL/6J to FVB) to minimize genetic heterogeneity of the mice, as described previously (6, 10). Briefly, mating male TG mice with female $MMP^{-/-}$ mice yielded TG or wild-type (WT) mice with $MMP^{+/-}$ (F1). Then we mated TG and WT mice with $MMP^{+/-}$ mice to obtain TG or WT mice with $MMP^{+/+}$, $MMP^{+/-}$, and $MMP^{-/-}$ (F2). To minimize the effect of genetic background, littermates were studied in each analysis. The study was approved by our Institutional Animal Research Committee and conformed to the animal care guidelines of the American Physiological Society.

MMPs and TIMPs. Myocardial MMP levels, including MMP-2 and MMP-9, were determined in the left ventricle (LV) from 12-wk-old female mice by gelatin zymography (8). The LV myocardial samples were homogenized (~30-s bursts) in 1 ml of an ice-cold extraction buffer containing cacodylic acid (10 mmol/l), NaCl (0.15 mol/l), $ZnCl_2$ (20 mmol/l), NaN_2 (1.5 mmol/l), and 0.01% Triton X-100 (pH 5.0). The homogenate was then centrifuged (4°C, 10 min, 10,000 *g*), and the supernatant was decanted and saved on ice. The pH levels of the samples were adjusted to 7.5 with Tris (1 mol/l). The final protein concentration of the myocardial extracts was determined using a standardized colorimetric assay. The extracted samples were aliquoted and stored at −80°C until the time of assay. The myocardial extracts were then directly loaded onto electrophoretic gels (SDS-PAGE) containing 1 mg/ml gelatin under nonreducing conditions. The myocardial extracts at a final protein content of 5 μg were loaded onto the gels using a 3:1 sample buffer (10% SDS, 4% sucrose, 0.25 mol/l Tris·Cl, and 0.1% bromphenol blue, pH 6.8). The gels were run at 15 mA/gel through the stacking phase (4%) and at 20 mA/gel for the separating phase (10%), while the running buffer temperature was maintained at 4°C. After SDS-PAGE, the gels were washed twice in 2.5% Triton X-100 for 30 min each, rinsed in water, and incubated for 24 h in a substrate buffer at 37°C (50 mmol/l Tris·HCl, 5 mmol/l, $CaCl_2$, and 0.02% NaN_3, pH 7.5). After incubation, the gels were stained with Coomassie brilliant blue R-250. The zymograms were digitized, and the size-fractionated bands, which indicated MMP proteolytic levels, were measured by integrated optical density in a rectangular region of interest.

The mRNA levels of myocardial MMPs, including MMP-1, MMP-2, MMP-3, MMP-8, and MMP-9, as well as TIMPs, including TIMP-1, TIMP-2, TIMP-3, and TIMP-4, were determined by multiprobe ribonuclease protection assay (RiboQuant, PharMingen). Each value was normalized to that of glyceraldehyde-3-phosphate dehydrogenase (GAPDH) in each template set as an internal control and then calculated as a ratio to $WT/MMP^{+/+}$.

Survival. Survival was analyzed in male and female $WT/MMP^{+/+}$, $WT/MMP^{-/-}$, $TG/MMP^{+/-}$, and $TG/MMP^{-/-}$ mice. During the study period, the cages were inspected daily to identify any deceased animals. All deceased mice were examined for the presence of pleural effusion (serous fluid within the chest wall cavity) in the postmortem examination. Because most of the male TG mice died earlier, we used 12-wk-old female mice for the subsequent analyses.

Echocardiographic and hemodynamic measurements. Echocardiographic studies were performed under light anesthesia with tribromoethanol-amylene hydrate (Avertin, 2.5% wt/vol, 8 μl/g ip) and spontaneous respiration as described previously (24). A two-dimensional parasternal short-axis view of the LV was obtained at the level of the papillary muscles. In general, the best views were obtained with the transducer lightly applied to the midportion of the upper left anterior chest wall. The transducer was then gently moved cephalad or caudad and angulated until desirable images were obtained. After confirmation that the imaging was on axis (on the basis of roundness of the LV cavity), two-dimensional targeted M-mode traces were recorded at a paper speed of 50 mm/s. Then a 1.4-Fr micromanometer-tipped catheter (Millar) was inserted into the right carotid artery and advanced into the LV to measure LV pressures. Our previous validation study showed that intra- and interobserver variabilities of our echocardiographic measurements for LV cavity dimensions and fractional shortening were small and that measurements made in the same animals on separate days were highly reproducible (24).

Histopathology. After in vivo echocardiographic and hemodynamic studies, the heart was excised and dissected into right ventricle and LV, including the septum. From the mid-LV transverse sections, 5-μm sections were cut and stained with hematoxylin and eosin and Masson's trichrome for determination of myocyte cross-sectional area and collagen volume fraction. They were stained also with picrosirius red for visualization of the interstitial collagen fibers.

Myocardial infiltration was quantified in hematoxylin-and-eosin-stained sections by determination of nuclear density (nuclei/mm^2) according to methods described previously (15, 21). Because it is difficult to differentiate inflammatory cells from myocytes and/or fibroblasts, all nuclei were included. In each animal, five independent high-power fields were analyzed. To further determine the number of macrophages, an immunohistochemical analysis using a specific antibody against mouse Mac-3 (BD Pharmingen) was performed.

Cytokine gene expression. To determine the myocardial gene expression of TNF-α as well as other proinflammatory cytokines, including regulated on activation, normal T cell expressed and secreted (RANTES), interleukin (IL)-6, IL-1β, transforming growth factor (TGF)-β, and monocyte chemoattractant protein (MCP)-1, ribonuclease protection assay was performed with 5 μg of total RNA isolated from LV tissue samples according to methods described previously (11).

Plasma cytokine and MMP levels. Plasma levels of TNF-α, as well as other cytokines, were measured with commercially available ELISA kits for mouse TNF-α, IL-6, IL-1β, and MCP-1 (Quantikine, R & D Systems). Plasma MMP-2 was also measured with commercially available ELISA kits (Quantikine). All assays were done in duplicate. Results were analyzed spectrophotometrically at a wavelength of 450 nm with a microtiter plate reader.

Statistical analysis. Values are means ± SE. A survival analysis was performed by the Kaplan-Meier method, and between-group difference in survival was tested by the log-rank test. Between-group comparisons of the means were performed by one-way ANOVA followed by *t*-tests. Bonferroni's correction was done for multiple comparisons of the means.

RESULTS

MMPs and TIMPs. Zymographic MMP-2 levels increased in TNF-α $TG/MMP^{+/+}$ compared with $WT/MMP^{+/+}$ mice (Fig. 1). As expected, MMP-2 activity was not detected in $WT/MMP^{-/-}$ and $TG/MMP^{-/-}$ mice. Importantly, the MMP-9 zymographic levels, even though they were faint in $WT/MMP^{+/+}$ mice, did not increase in $WT/MMP^{-/-}$ mice. They significantly increased in the TNF-α TG groups; however, no difference was seen between $TG/MMP^{+/+}$ and $TG/MMP^{-/-}$ mice.

Again, the MMP-2 mRNA levels significantly increased in TNF-α $TG/MMP^{+/+}$ compared with $WT/MMP^{+/+}$ mice (Fig. 2). This increase was completely prevented in $TG/MMP^{-/-}$ mice. The MMP-9 mRNA levels also increased in the TNF-α TG groups; however, no difference was seen between $TG/MMP^{+/+}$ and $TG/MMP^{-/-}$ mice. These results were consistent with those observed in gelatin zymography (Fig. 1). Other MMPs, including MMP-1, MMP-3, and MMP-8, were not altered in these mice (Fig. 2). The changes in TIMPs (TIMP-1, TIMP-2, TIMP-3, and TIMP-4) were comparable between $TG/MMP^{+/+}$ and $TG/MMP^{-/-}$ mice.

Survival. Survival rate was shorter for male $TG/MMP^{-/-}$ than $TG/MMP^{+/+}$ mice (Fig. 3). Although MMP-2 gene ab-

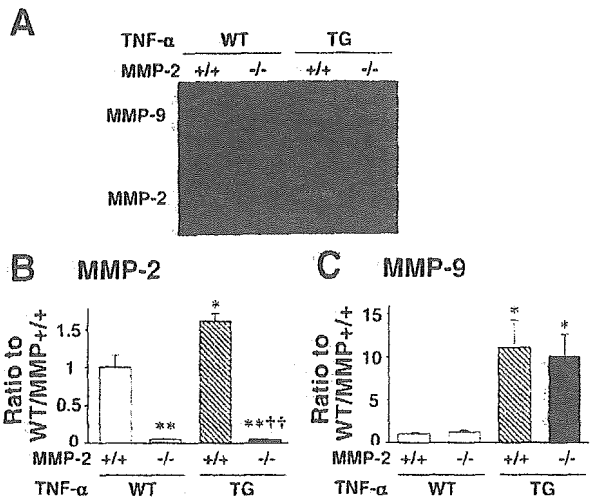

Fig. 1. *A*: representative gelatin zymography of left ventricle (LV) from wild-type (WT) mice with wild matrix metalloproteinase-2 (WT/MMP$^{+/+}$), WT mice with MMP-2 knockout (KO) (WT/MMP$^{-/-}$), TNF-α transgenic (TG) mice with MMP-2 (TG/MMP$^{+/+}$), and TNF-α TG mice with MMP-2 KO (TG/MMP$^{-/-}$). *B* and *C*: densitometric analysis of MMP-2 and MMP-9 zymographic activity (n = 3/group). Samples from WT/MMP$^{+/+}$ mice were run concurrently on the same gel. Values are means ± SE. *P < 0.05; **P < 0.01 vs. WT/MMP$^{-/-}$. ††P < 0.01 vs. TG/MMP$^{+/+}$.

lation was also observed in female mice, it has less effect on survival. These observations of gender differences in survival were consistent with results from a previous study (14), which demonstrated that such gender differences might be due to higher expression of TNF-α receptors in the myocardium of male TG mice, because the extent of myocardial expression of TNF-α was comparable in both genders (14). All the TG mice that died spontaneously developed cardiac dilatation and pleural effusion, suggesting that they died of heart failure. Because most of the male TG mice died earlier, we used surviving 12-wk-old female mice for the subsequent analyses.

Echocardiography and hemodynamics. The echocardiographic and hemodynamic data of the surviving 12-wk-old

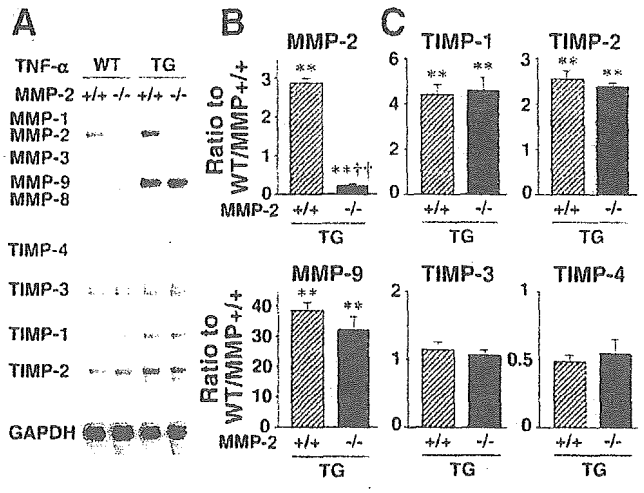

Fig. 2. *A*: representative image of myocardial gene expression of MMPs and tissue inhibitors of MMPs (TIMPs). *B* and *C*: densitometric analysis of MMP and TIMP gene expression in TG/MMP$^{+/-}$ (n = 7) and TG/MMP$^{-/-}$ (n = 7) mice. Each value was normalized to that of GAPDH in each template set as an internal control and expressed as ratio to WT/MMP$^{+/-}$ (n = 6). Values are means ± SE. **P < 0.01 vs. WT/MMP$^{+/+}$. ††P < 0.01 vs. TG/MMP$^{+/-}$.

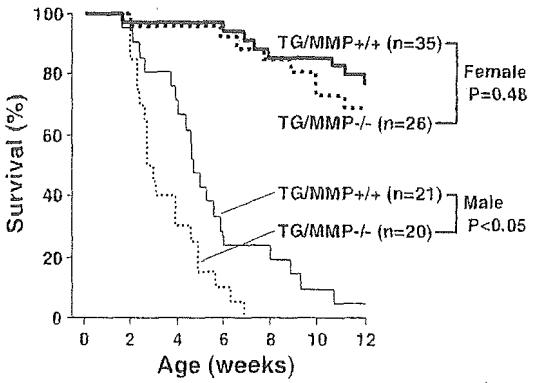

Fig. 3. Kaplan-Meier survival analysis of survival in male TG/MMP$^{+/+}$ (n = 21) and TG/MMP$^{-/-}$ (n = 20) and female TG/MMP$^{+/-}$ (n = 35) and TG/MMP$^{-/-}$ (n = 26) mice.

female mice are shown in Table 1. Presence or absence of the MMP-2 gene did not affect baseline echocardiographic parameters in WT mice. LV end-diastolic diameter was significantly greater, and fractional shortening was significantly less in TG/MMP$^{+/+}$ than in WT mice. TG/MMP$^{-/-}$ mice exerted more impaired LV contractile function than TG/MMP$^{+/+}$ mice.

There was no significant difference in heart rate or LV end-diastolic pressure (EDP) between WT/MMP$^{+/+}$ and WT/MMP$^{-/-}$ mice. LV EDP increased slightly, but significantly, in TG/MMP$^{+/+}$ mice and further increased in TG/MMP$^{-/-}$ mice. Consistent with LV EDP, pleural effusion was observed only in TG/MMP$^{-/-}$ mice. On the basis of these results, the exacerbation of heart failure might contribute to premature death in TG/MMP$^{-/-}$ mice.

Histopathology. We examined the histopathology of the heart from 12-wk-old female mice. LV weight was significantly increased in the TG groups compared with the WT groups (Table 1); however, LV weight did not differ between TG/MMP$^{+/+}$ and TG/MMP$^{-/-}$ mice. Furthermore, myocyte cross-sectional area and collagen volume fraction were increased in TNF-α TG groups (Fig. 4, *A* and *B*). However, the extent of these histopathological changes was comparable between TG/MMP$^{+/+}$ and TG/MMP$^{-/-}$ mice. Moreover, in picrosirius red-stained sections, the structure of the interstitial collagen fibers was similar between TG/MMP$^{+/+}$ and TG/MMP$^{-/-}$ mice (Fig. 4*C*), indicating that selective disruption of the MMP-2 gene did not alter collagen content or structure in this mouse model.

The number of infiltrating interstitial cells in the myocardium was greater in TNF-α TG than in WT mice (Fig. 5). The extent of infiltration was significantly greater in TG/MMP$^{-/-}$ than TG/MMP$^{+/+}$ mice. Macrophages infiltrated into the myocardium from TG mice, and, importantly, selective MMP-2 ablation further augmented their infiltration (Fig. 6).

Cytokine gene expression. TNF-α gene expression was significantly upregulated in the TNF-α TG myocardium (Fig. 7). In addition, overexpression of the TNF-α gene increased expression of other cytokines and chemokines, including RANTES, IL-6, IL-1β, and MCP-1, indicating that overexpression of TNF-α induced "downstream" cytokines and chemokines in this model. Importantly, upregulation of TNF-α was not altered by ablation of the MMP-2 gene. Similarly, MMP-2 gene ablation in TG mice had no significant effects on myo-

Table 1. *Characteristics of animal models*

	WT/MMP$^{+/+}$ (n = 15)	WT/MMP$^{-/-}$ (n = 15)	TG/MMP$^{+/+}$ (n = 15)	TG/MMP$^{-/-}$ (n = 17)
Echocardiographic data				
Heart rate, beats/min	450±11	446±10	452±12	453±11
LV EDD, mm	3.4±0.1	3.3±0.1	4.3±0.1*	4.5±0.2*
Fractional shortening, %	37.4±0.8	36.8±0.7	26.7±0.9*	22.9±1.3*†
Hemodynamic data				
Heart rate, beats/min	471±10	469±10	460±9	459±8
LV EDP, mmHg	0.5±0.7	0.2±0.3	1.5±0.7*	7.2±2.5*†
Organ weight data				
Body wt, g	20.7±0.5	19.2±0.4	21.7±0.4	20.7±0.5
LV wt/body wt, mg/g	3.0±0.1	2.9±0.0	3.8±0.1*	3.9±0.2*
Pleural effusion, %			0	18

Values are means ± SE. WT/MMP$^{+/+}$, wild-type mice with matrix metalloproteinase-2 (MMP-2); WT/MMP$^{-/-}$, wild-type mice with MMP-2 knockout; TG/MMP$^{+/+}$, transgene (TG) mice with cardiac overexpression of TNF-α with MMP-2; TG/MMP$^{-/-}$, TG mice with cardiac overexpression of TNF-α with MMP-2 knockout; LV, left ventricular; EDD, end-diastolic diameter; EDP, end-diastolic pressure. *P < 0.01 vs. WT/MMP$^{+/+}$. †P < 0.05 vs. TG/MMP$^{+/+}$.

cardial mRNA levels of other cytokines/chemokines, indicating that the decline in survival and LV function in TG/MMP$^{-/-}$ mice was not due to enhancement of myocardial cytokine/chemokine expression by selective disruption of the MMP-2 gene.

Plasma cytokine and MMP levels. Plasma levels of TNF-α, as well as other cytokines, were below detection in the four groups of animals (Table 2), consistent with previous studies demonstrating that the TNF-α TG transcripts were limited to the heart (16). As expected, plasma levels of MMP-2 were very low in MMP-2 KO mice. Plasma MMP-2 was comparable between WT/MMP$^{+/+}$ and TG/MMP$^{+/+}$ mice.

DISCUSSION

In the present study, we demonstrated that selective disruption of the MMP-2 gene exacerbated survival and LV function in TG mice with cardiac-specific overexpression of TNF-α. Disruption of the MMP-2 gene did not alter myocardial hypertrophy and interstitial fibrosis but exacerbated inflammatory cell infiltration. These results indicate that MMP-2 plays a protective role against myocardial inflammation and dysfunction in cytokine-induced cardiomyopathy.

Consistent with previous studies (17, 18), MMP-2 mRNA and activities were upregulated in myocardium from animals with TNF-α-induced cardiomyopathy (Figs. 1 and 2). Although the mechanisms responsible for this activation remain to be determined, cellular constituents of cardiac muscle, including fibroblasts, inflammatory cells, and myocytes, are known to be capable of expressing MMP-2 in response to specific stimuli (25). Activation of MMPs may be involved in the remodeling process of the failing heart by provoking alterations of the ECM (4, 8, 20, 23, 26, 27). Indeed, MMP-9 disruption reduced myocardial remodeling and improved LV function and survival rate after myocardial infarction (9). Similarly, MMP-2 ablation inhibited cardiac rupture and remodeling after myocardial infarction (8).

The present study investigated the long-term effects of selective MMP-2 gene disruption on development of TNF-α-induced cardiomyopathy. We employed KO mice, because selective MMP-2 inhibitors are not available and "selective" MMP-2 disruption is possible only with a KO mouse model. As expected, no MMP-2 expression was observed in myocardium from WT/MMP$^{-/-}$ and TG/MMP$^{-/-}$ mice (Figs. 1 and

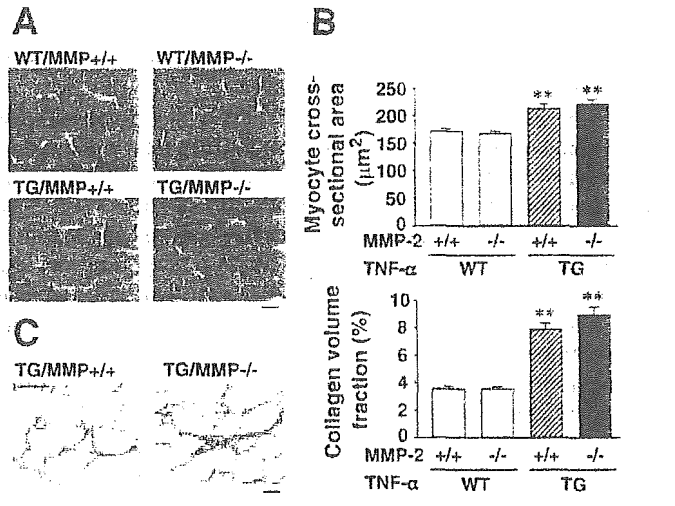

Fig. 4. *A*: representative high-power photomicrographs of Masson's trichrome-stained LV cross sections from WT/MMP$^{+/+}$, WT/MMP$^{-/-}$, TG/MMP$^{+/+}$, and TG/MMP$^{-/-}$ mice. Scale bar, 10 μm. *B*: summary data of myocyte cross-sectional area and collagen volume fraction by histopathological analysis of LV tissue sections (n = 6/group). Values are means ± SE. **P < 0.01 vs. WT/MMP$^{+/+}$. *C*: representative high-power photomicrographs of picrosirius red-stained LV cross sections from TG/MMP$^{+/+}$ and TG/MMP$^{-/-}$ mice. Scale bar, 10 μm.

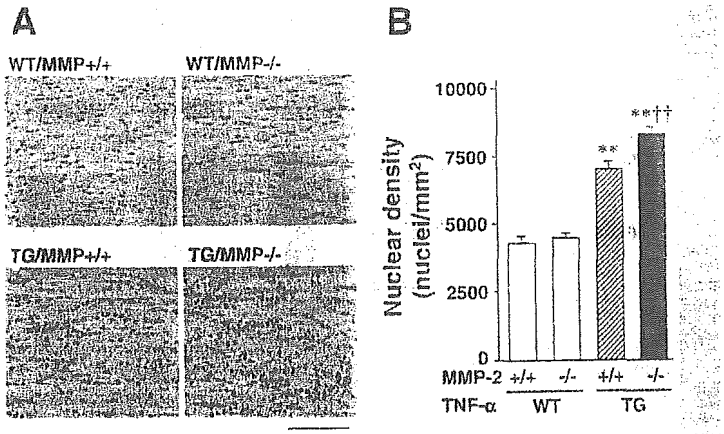

Fig. 5. *A*: representative photomicrographs of hematoxylin-and-eosin-stained LV sections from WT/MMP$^{+/+}$, WT/MMP$^{-/-}$, TG/MMP$^{+/+}$, and TG/MMP$^{-/-}$ mice. Scale bar, 100 μm. *B*: summary data for nuclear density of infiltrating cells (n = 6/group). Values are means ± SE. **P < 0.01 vs. WT/MMP$^{+/+}$. ††P < 0.01 vs. TG/MMP$^{+/+}$.

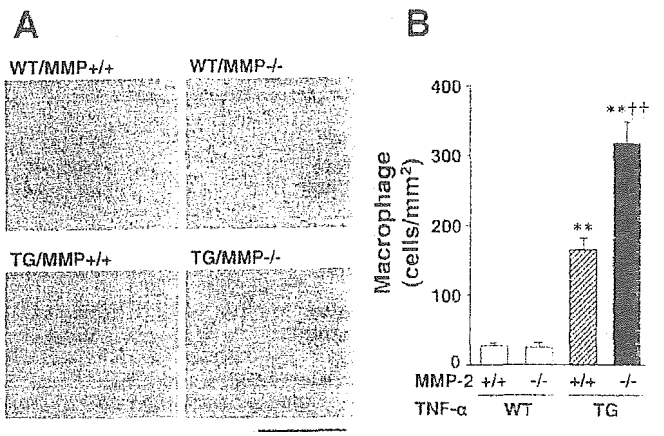

Fig. 6. *A*: representative photomicrographs of anti-Mac-3 antibody-stained LV sections from WT/MMP$^{+/+}$, WT/MMP$^{-/-}$, TG/MMP$^{+/+}$, and TG/MMP$^{-/-}$ mice. Scale bar, 100 μm. *B*: summary data for density of Mac-3-positive cells (n = 5/group). Values are means ± SE. **P < 0.01 vs. WT/MMP$^{+/+}$. ††P < 0.01 vs. TG/MMP$^{+/+}$.

2). We had expected that MMP-2 disruption could ameliorate cardiac ECM remodeling and dysfunction in TNF-α TG mice and prolong survival. On the contrary, selective blockade of the MMP-2 gene exacerbated LV contractile dysfunction and failure (Table 1) and even shortened survival (Fig. 3), suggesting that myocardial induction of MMP-2 may play a protective role against the development of cytokine-induced cardiomyopathy.

The most striking finding of the present study was an increase in inflammatory cell recruitment into the myocardium seen in MMP-2 KO mice due to overexpression of TNF-α in the heart (Figs. 5 and 6). Even though the pathophysiological significance of cellular infiltrates in myocardial remodeling and failure remains mostly speculative in this model, the observed increase in inflammation might exacerbate myocardial contractile and structural defects, which could lead to premature death

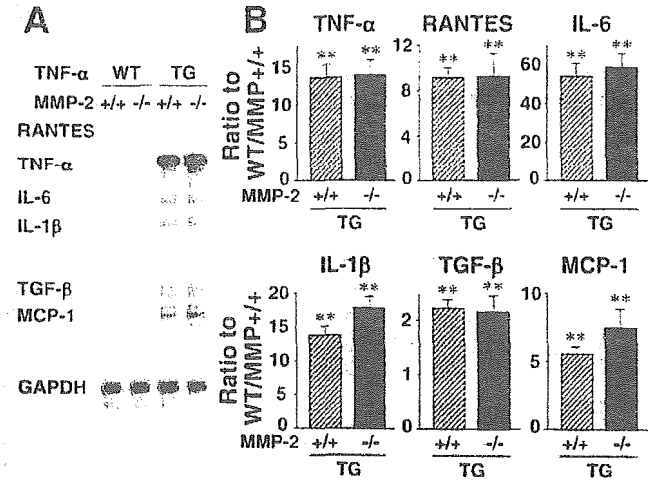

Fig. 7. *A*: myocardial gene expression of proinflammatory cytokines and chemokines from WT/MMP$^{+/+}$, WT/MMP$^{-/-}$, TG/MMP$^{+/+}$, and TG/MMP$^{-/-}$ mice. *B*: densitometric analysis of gene expression in myocardium from TG/MMP$^{+/+}$ (n = 7) and TG/MMP$^{-/-}$ (n = 6) mice. Each value was normalized to that of GAPDH in each template set as an internal control and expressed as ratio to WT/MMP$^{+/+}$ (n = 6). MCP, monocyte chemoattractant protein; TGF, transforming growth factor; RANTES, regulated on activation, normal T cell expressed and secreted. Values are means ± SE. **P < 0.01 vs. WT/MMP$^{+/+}$.

Table 2. *Plasma levels of cytokines and MMPs*

	WT/MMP$^{+/+}$	WT/MMP$^{-/-}$	TG/MMP$^{+/+}$	TG/MMP$^{-/-}$
Cytokines/chemokines				
TNF-α, pg/ml	ND	ND	ND	ND
IL-6, pg/ml	9.0±0.2	9.0±0.8	9.0±0.6	10.4±2.5
IL-1β, pg/ml	ND	ND	ND	ND
MCP-1, pg/ml	20.7±10.2	8.3±3.2	17.3±3.3	24.9±6.3
MMP				
MMP-2, ng/ml	60.9±3.0	0.9±0.2*	63.2±2.5	0.8±0.2*

Values are means ± SE; n = 5. ND, not detectable; MCP, monocyte chemoattractant protein. *P < 0.01 vs. WT/MMP$^{+/+}$.

in TG/MMP$^{-/-}$ mice. Several potential mechanisms of MMP-2 deletion are responsible for exacerbating cellular inflammation in TNF-α TG hearts. One possible mechanism is a further increase in expression of the TNF-α gene in TG/MMP$^{-/-}$ mice and the resultant enhancement of inflammation. However, this possibility is less likely, because the gene expression of cytokines, TNF-α and MCP-1, was not altered by selective disruption of the MMP-2 gene (Fig. 7), perhaps in part because expression of TNF-α in TG mice is driven by α-myosin heavy chain promoter, which is supposed to be MMP-2 independent. Another possibility is that MMP-2 might alter the milieu of the ECM, which could accelerate the infiltration of cells. In the present study, no significant changes were observed in collagen deposition between TG/MMP$^{+/+}$ and TG/MMP$^{-/-}$ mice (Fig. 4). Therefore, exacerbation of myocardial inflammation in TG/MMP$^{-/-}$ mice was not due to impairment of interstitial collagen formation and/or structure.

Theoretically, an increase in MMP activity would result in a decrease in the MMP substrate, collagen, whereas inhibition of MMP-2 would result in an increase in collagen. However, in agreement with previous studies (18), the present study demonstrated that an increase in MMP-2 activity was accompanied by an increase in fibrosis in TNF-α TG mice (Fig. 4). Moreover, selective disruption of the MMP-2 gene did not alter these changes in interstitial fibrosis. The present study could not provide a definite explanation for these paradoxical findings, perhaps because total ECM collagen content is a complex function of synthesis and degradation.

Although the functional role of MMP-2 in this aspect and its significance in myocardial inflammation remain unknown, on the basis of a previous study by Heymans et al. (9), we could not exclude the possibility that deletion of the MMP-2 gene might alter ECM components other than collagens, disrupt the alignment of myocytes with the ECM or degrade the ECM surrounding the myocytes, and promote the further progression of inflammatory cell migration into the interstitial space. MMPs have been shown to facilitate inflammatory cell recruitment (7). However, the present study does not provide a direct proof for the cause-and-effect relation between the increase in cellular infiltration and the exacerbation of heart failure, and further investigation is clearly needed.

The results of the present study are consistent with those of previous studies of MMP-2 gene ablation in other models of tissue inflammation (3, 13). Disruption of the MMP-2 gene exacerbated allergic lung inflammation and increased lethal susceptibility to asphyxiation in a mouse model of asthma (3). Furthermore, Itoh et al. (13) demonstrated an increase in severity of arthritis in association with tissue inflammation in

MMP-2 KO mice. These results indicate that MMP-2 suppressed the development of inflammatory disease. Therefore, TNF-α overexpression and MMP-2 deletion might synergistically activate the cellular inflammatory response in the heart, which could further damage cardiac function.

The present study could not demonstrate the long-term beneficial effects of MMP-2 deletion on the decline in LV systolic function in TNF-α-induced cardiomyopathy. These findings are in contrast to those from a previous study, in which broad-spectrum MMP inhibition could ameliorate myocardial dysfunction in TNF-α TG mice (18). The MMP inhibitor batimastat was found to reduce myocardial hypertrophy and diastolic dysfunction. Even though it is difficult to compare the two studies directly because of the broad-spectrum action of the MMP inhibitor used by Li et al. (18), these studies suggest that MMP-2 has a complex role in maintaining the physiological function of the heart, and information about the action of individual MMPs with the use of such an inhibitor is limited. The most effective way to evaluate the contribution of the specific MMP and obtain direct evidence for a role of MMP in heart failure is through gene manipulation, as employed in the present study. Whatever the mechanisms are, MMP-2 could protect the heart by inhibiting acceleration of interstitial inflammatory infiltration in this model. The disparity between selective and nonselective inhibition of MMP-2 may have important implications in the development of pharmacological agents for the treatment of heart failure. These findings may further draw attention to treatment of heart failure by using the nonselective, broad-spectrum MMP-2 inhibitor.

There are several limitations to be acknowledged in this study. *1*) We examined only female mice for physiological, pathological, and biochemical analyses, because most male TG mice died before 12 wk of age, when these analyses were performed. As a result, we are not certain whether selective disruption of the MMP-2 gene exacerbates myocardial inflammation and dysfunction even in male TNF-α TG mice. *2*) Even though in vivo assessment of LV function with echocardiography is feasible and reproducible in the mouse, it might be difficult to interpret the indexes in dilated LV. However, our validation study has shown that intra- and interobserver variabilities of our echocardiographic measurements for LV cavity dimensions and fractional shortening were small and that measurements in the same animals on separate days were highly reproducible (24). Therefore, our technique could be considered to allow for a noninvasive assessment of LV structure. *3*) The heart rates in the present study (450–470 beats/min) were lower than those measured in conscious mice (600 beats/min). Therefore, the LV size and function results might be greatly influenced by differences in anesthetic regimens and experimental conditions, such as heart rate. *4*) Although the present study employed the conventional gelatin zymography method to analyze MMP activities, as in a previous study (8), two-dimensional zymography is essential, especially to ascertain the existence of plasmin in the 66-kDa MMP complex (28). *5*) We assessed TGF-β, which has been well established to be involved in ECM remodeling in heart failure, in the present study. Further studies on TGF-α are also needed, because it plays an important role in cell proliferation and differentiation.

In summary, selective disruption of the MMP-2 gene exacerbated myocardial inflammation and dysfunction in TNF-α-induced cardiomyopathy. Thus myocardial expression of MMP-2 may play a protective role in the development of congestive heart failure in cytokine-induced cardiomyopathy.

GRANTS

This study was supported in part by Ministry of Education, Science, and Culture Grants 09670724, 12670676, and 14370230. A part of this study was conducted at the Kyushu University Station for Collaborative Research I and II.

REFERENCES

1. **Carlyle WC, Jacobson AW, Judd DL, Tian B, Chu C, Hauer KM, Hartman MM, and McDonald KM.** Delayed reperfusion alters matrix metalloproteinase activity and fibronectin mRNA expression in the infarct zone of the ligated rat heart. *J Mol Cell Cardiol* 29: 2451–2463, 1997.
2. **Cheung PY, Sawicki G, Wozniak M, Wang W, Radomski MW, and Schulz R.** Matrix metalloproteinase-2 contributes to ischemia-reperfusion injury in the heart. *Circulation* 101: 1833–1839, 2000.
3. **Corry DB, Rishi K, Kanellis J, Kiss A, Song LZ, Xu J, Feng L, Werb Z, and Kheradmand F.** Decreased allergic lung inflammatory cell egression and increased susceptibility to asphyxiation in MMP2-deficiency. *Nat Immunol* 3: 347–353, 2002.
4. **Ducharme A, Frantz S, Aikawa M, Rabkin E, Lindsey M, Rohde LE, Schoen FJ, Kelly RA, Werb Z, Libby P, and Lee RT.** Targeted deletion of matrix metalloproteinase-9 attenuates left ventricular enlargement and collagen accumulation after experimental myocardial infarction. *J Clin Invest* 106: 55–62, 2000.
5. **Feldman AM, Combes A, Wagner D, Kadakomi T, Kubota T, Li YY, and McTiernan C.** The role of tumor necrosis factor in the pathophysiology of heart failure. *J Am Coll Cardiol* 35: 537–544, 2000.
6. **Funakoshi H, Kubota T, Kawamura N, Machida Y, Feldman AM, Tsutsui H, Shimokawa H, and Takeshita A.** Disruption of inducible nitric oxide synthase improves β-adrenergic inotropic responsiveness but not the survival of mice with cytokine-induced cardiomyopathy. *Circ Res* 90: 959–965, 2002.
7. **Haas TL and Madri JA.** Extracellular matrix-driven matrix metalloproteinase production in endothelial cells: implications for angiogenesis. *Trends Cardiovasc Med* 9: 70–77, 1999.
8. **Hayashidani S, Tsutsui H, Ikeuchi M, Shiomi T, Matsusaka H, Kubota T, Imanaka-Yoshida K, Itoh T, and Takeshita A.** Targeted deletion of MMP-2 attenuates early LV rupture and late remodeling after experimental myocardial infarction. *Am J Physiol Heart Circ Physiol* 285: H1229–H1235, 2003.
9. **Heymans S, Luttun A, Nuyens D, Theilmeier G, Creemers E, Moons L, Dyspersin GD, Cleutjens JP, Shipley M, Angellilo A, Levi M, Nube O, Baker A, Keshet E, Lupu F, Herbert JM, Smits JF, Shapiro SD, Baes M, Borgers M, Collen D, Daemen MJ, and Carmeliet P.** Inhibition of plasminogen activators or matrix metalloproteinases prevents cardiac rupture but impairs therapeutic angiogenesis and causes cardiac failure. *Nat Med* 5: 1135–1142, 1999.
10. **Higuchi Y, McTiernan CF, Frye CB, McGowan BS, Chan TO, and Feldman AM.** Tumor necrosis factor receptors 1 and 2 differentially regulate survival, cardiac dysfunction, and remodeling in transgenic mice with tumor necrosis factor-α-induced cardiomyopathy. *Circulation* 109: 1892–1897, 2004.
11. **Ikeuchi M, Tsutsui H, Shiomi T, Matsusaka H, Matsushima S, Wen J, Kubota T, and Takeshita A.** Inhibition of TGF-β signaling exacerbates early cardiac dysfunction but prevents late remodeling after infarction. *Cardiovasc Res* 64: 526–535, 2004.
12. **Itoh T, Ikeda T, Gomi H, Nakao S, Suzuki T, and Itohara S.** Unaltered secretion of β-amyloid precursor protein in gelatinase A (matrix metalloproteinase 2)-deficient mice. *J Biol Chem* 272: 22389–22392, 1997.
13. **Itoh T, Matsuda H, Tanioka M, Kuwabara K, Itohara S, and Suzuki R.** The role of matrix metalloproteinase-2 and matrix metalloproteinase-9 in antibody-induced arthritis. *J Immunol* 169: 2643–2647, 2002.
14. **Kadokami T, McTiernan CF, Kubota T, Frye CS, and Feldman AM.** Sex-related survival differences in murine cardiomyopathy are associated with differences in TNF-receptor expression. *J Clin Invest* 106: 589–597, 2000.
15. **Kubota T, Bounoutas GS, Miyagishima M, Kadokami T, Sanders VJ, Bruton C, Robbins PD, McTiernan CF, and Feldman AM.** Soluble tumor necrosis factor receptor abrogates myocardial inflammation but not hypertrophy in cytokine-induced cardiomyopathy. *Circulation* 101: 2518–2525, 2000.

16. **Kubota T, McTiernan CF, Frye CS, Slawson SE, Lemster BH, Koretsky AP, Demetris AJ, and Feldman AM.** Dilated cardiomyopathy in transgenic mice with cardiac-specific overexpression of tumor necrosis factor-α. *Circ Res* 81: 627–635, 1997.
17. **Li YY, Feng YQ, Kadokami T, McTiernan CF, Draviam R, Watkins SC, and Feldman AM.** Myocardial extracellular matrix remodeling in transgenic mice overexpressing tumor necrosis factor-α can be modulated by anti-tumor necrosis factor-α therapy. *Proc Natl Acad Sci USA* 97: 12746–12751, 2000.
18. **Li YY, Kadokami T, Wang P, McTiernan CF, and Feldman AM.** MMP inhibition modulates TNF-α transgenic mouse phenotype early in the development of heart failure. *Am J Physiol Heart Circ Physiol* 282: H983–H989, 2002.
19. **Li YY, McTiernan CF, and Feldman AM.** Proinflammatory cytokines regulate tissue inhibitors of metalloproteinases and disintegrin metalloproteinase in cardiac cells. *Cardiovasc Res* 42: 162–172, 1999.
20. **Lindsey ML, Gannon J, Aikawa M, Schoen FJ, Rabkin E, Lopresti-Morrow L, Crawford J, Black S, Libby P, Mitchell PG, and Lee RT.** Selective matrix metalloproteinase inhibition reduces left ventricular remodeling but does not inhibit angiogenesis after myocardial infarction. *Circulation* 105: 753–758, 2002.
21. **Machida Y, Kubota T, Kawamura N, Funakoshi H, Ide T, Utsumi H, Li YY, Feldman AM, Tsutsui H, Shimokawa H, and Takeshita A.** Overexpression of tumor necrosis factor-α increases production of hydroxyl radical in murine myocardium. *Am J Physiol Heart Circ Physiol* 284: H449–H455, 2003.
22. **Mann DL and Young JB.** Basic mechanisms in congestive heart failure. Recognizing the role of proinflammatory cytokines. *Chest* 105: 897–904, 1994.
23. **Rohde LE, Ducharme A, Arroyo LH, Aikawa M, Sukhova GH, Lopez-Anaya A, McClure KF, Mitchell PG, Libby P, and Lee RT.** Matrix metalloproteinase inhibition attenuates early left ventricular enlargement after experimental myocardial infarction in mice. *Circulation* 99: 3063–3070, 1999.
24. **Shiomi T, Tsutsui H, Hayashidani S, Suematsu N, Ikeuchi M, Wen J, Ishibashi M, Kubota T, Egashira K, and Takeshita A.** Pioglitazone, a peroxisome proliferator-activated receptor-γ agonist, attenuates left ventricular remodeling and failure after experimental myocardial infarction. *Circulation* 106: 3126–3132, 2002.
25. **Siwik DA, Chang DL, and Colucci WS.** Interleukin-1β and tumor necrosis factor-α decrease collagen synthesis and increase matrix metalloproteinase activity in cardiac fibroblasts in vitro. *Circ Res* 86: 1259–1265, 2000.
26. **Spinale FG, Coker ML, Thomas CV, Walker JD, Mukherjee R, and Hebbar L.** Time-dependent changes in matrix metalloproteinase activity and expression during the progression of congestive heart failure: relation to ventricular and myocyte function. *Circ Res* 82: 482–495, 1998.
27. **Thomas CV, Coker ML, Zellner JL, Handy JR, Crumbley AJ III, and Spinale FG.** Increased matrix metalloproteinase activity and selective upregulation in LV myocardium from patients with end-stage dilated cardiomyopathy. *Circulation* 97: 1708–1715, 1998.
28. **Tyagi SC, Kumar SG, Haas SJ, Reddy HK, Voelker DJ, Hayden MR, Demmy TL, Schmaltz RA, and Curtis JJ.** Post-transcriptional regulation of extracellular matrix metalloproteinase in human heart end-stage failure secondary to ischemic cardiomyopathy. *J Mol Cell Cardiol* 28: 1415–1428, 1996.
29. **Wang W, Schulze CJ, Suarez-Pinzon WL, Dyck JR, Sawicki G, and Schulz R.** Intracellular action of matrix metalloproteinase-2 accounts for acute myocardial ischemia and reperfusion injury. *Circulation* 106: 1543–1549, 2002.

Hypertension
JOURNAL OF THE AMERICAN HEART ASSOCIATION

Inhibition of Rho-Kinase in the Nucleus Tractus Solitarius Enhances Glutamate Sensitivity in Rats

Koji Ito, Yoshitaka Hirooka, Nobuaki Hori, Yoshikuni Kimura, Yoji Sagara, Hiroaki Shimokawa, Akira Takeshita and Kenji Sunagawa

Hypertension published online Jul 5, 2005;
DOI: 10.1161/01.HYP.0000177119.23178.05
Hypertension is published by the American Heart Association. 7272 Greenville Avenue, Dallas, TX 72514
 Print ISSN: 0194-911X. Online ISSN: 1524-4563

Inhibition of Rho-Kinase in the Nucleus Tractus Solitarius Enhances Glutamate Sensitivity in Rats

Koji Ito, Yoshitaka Hirooka, Nobuaki Hori, Yoshikuni Kimura, Yoji Sagara, Hiroaki Shimokawa, Akira Takeshita, Kenji Sunagawa

Abstract—The Rho/Rho–kinase pathway in the central nervous system is involved in the maintenance of dendritic spines, which form the postsynaptic contact sites of excitatory synapses. Inhibition of the Rho–kinase pathway in neuron promotes dendritic spines or branches. In contrast, activation of the Rho/Rho–kinase pathway reduces dendritic spines or branches. Recent studies suggest that morphological changes of dendritic spines occur rapidly, and spine morphology is associated with glutamate sensitivity. The aim of the present study was to determine whether Rho-kinase activity affects glutamate sensitivity in the nucleus tractus solitarii (NTS) of Wistar-Kyoto rats (WKY) and spontaneously hypertensive rats (SHR). We first examined the effects of unilateral glutamate injection in the NTS. There was a significantly smaller decrease in arterial pressure in SHR than in WKY. We then examined the depressor responses evoked by unilateral glutamate injection into the NTS after preinjection of Y-27632, a specific Rho-kinase inhibitor. Preinjection of Y-27632 enhanced the glutamate response in both strains. However, the magnitude of the augmentation was significantly greater in SHR than in WKY. Furthermore, we recorded single-unit activity of NTS neurons from medulla brain slice preparations. *N*-methyl-D-aspartate (NMDA) or α-amino-3-hydroxy-5-methyl-4-isoxazolepropionate (AMPA) was applied iontophoretically to the recorded neurons, and neuronal activity was recorded before and after Y-27632 perfusion. Y-27632 perfusion increased the response to NMDA and AMPA. These results suggest that inhibition of Rho-kinase activity in the NTS enhances glutamate sensitivity in WKY and SHR and might improve impaired glutamate sensitivity in SHR. (***Hypertension.* 2005;46:1-7.**)

Key Words: blood pressure ■ autonomic nervous system ■ amino acid ■ rats, spontaneously hypertensive ■ central nervous system

The Rho/Rho–kinase pathway regulates myosin light chain phosphorylation and contributes to smooth muscle contraction.[1–3] Y-27632, a selective Rho-kinase inhibitor, reduces arterial pressure in rat models of hypertension,[4] and Rho-kinase activity is enhanced in hypertensive blood vessels.[5,6] Thus, the Rho/Rho–kinase pathway is involved in the peripheral mechanisms of hypertension. We reported previously that Rho-kinase is present in the brain stem and maintains arterial pressure via the sympathetic nervous system, and that activation of the Rho/Rho–kinase pathway in the brain stem might contribute to the central mechanisms of hypertension.[7,8] Furthermore, inhibition of Rho-kinase in the nucleus tractus solitarii (NTS) enhances baroreflex control of heart rate (HR) in Wistar-Kyoto rats (WKY) and spontaneously hypertensive rats (SHR), probably because of a cardiac sympathoinhibitory effect.[9]

The Rho/Rho–kinase pathway in the central nervous system is involved in the maintenance of dendritic spines.[10] Dendritic spines form the postsynaptic contact sites of excitatory synapses in the central nervous system.[11] Inhibition of the Rho-kinase pathway in neuron promotes dendritic spines or branches. In contrast, activation of the Rho/Rho–kinase pathway reduces dendritic spines or branches.[10,12] Recent studies suggest that morphological changes of dendritic spines occur rapidly,[13] and spine morphology is associated with glutamate sensitivity.[14] Furthermore, GTPase-activating protein p250GAP, which is highly expressed in the brain, coexists with RhoA in dendritic spines and is involved in *N*-methyl-D-aspartate (NMDA) glutamate receptor activity-dependent actin reorganization in dendritic spines.[15] Furthermore, Rho-kinase in the brain stem contributes to arterial blood pressure regulation and baroreflex function.[7–9] The physiological role of Rho-kinase in neurons has not been clarified; however, these findings led to the hypothesis that inhibition of the Rho/Rho–kinase pathway in the NTS affects synaptic transmission, particularly in the excitatory synapses, via an enhanced response to glutamate. Therefore, the aim of the present study was to determine whether the Rho/Rho–kinase pathway in the NTS affects glutamate sensitivity in the NTS. For this purpose, we examined depressor responses

Received January 6, 2005; first decision January 20, 2005; revision accepted June 6, 2005.

From the Departments of Cardiovascular Medicine (K.I., Y.H., Y.K., Y.S., H.S., A.T., K.S.) and Pharmacology (N.H.), Kyushu University Graduate School of Medical Sciences, Fukuoka, Japan.

Correspondence to Yoshitaka Hirooka, MD, PhD, FAHA, Department of Cardiovascular Medicine, Kyushu University Graduate School of Medical Sciences, 3-1-1 Maidashi, Higashi-ku, Fukuoka 812-8582, Japan. E-mail hyoshi@cardiol.med.kyushu-u.ac.jp

Hypertension **is available at http://www.hypertensionaha.org** **DOI: 10.1161/01.HYP.0000174328.06691.e9**